Anonymous Referee #1

Received and published: 20 February 2019

In the manuscript "Photolytically-Generated Sulfuric Acid and Particle Formation: Dependence on Precursor Species", the authors Hanson et al. present a set of well carried out flow tube experiments of sulfuric acid formation and new-particle formation. The experiments, accompanied by model simulations, are explained very well, and the analysis and interpretation of the obtained data is convincing (though I feel could be streamlined a bit). I especially like the good level of detail in section 2 ("Methods"). The paper concludes with a comparison of the experimental results to existing literature and discusses the effects mainly of adding base compounds (ammonia and dimethylamine) to the system – not only in the authors' experiments, but at this kind of new-particle formation experiments in general. In total, I think this is interesting work that deserves publication. I did find several points where the manuscript could be substantially improved or at least clarified. I think that overall these "main comments" concern details of how the results are presented, but I believe they need to be considered prior to acceptance. Finally, although this is a convincing, interesting and detailed study of flow tube SA nucleation (and including an interesting application of the authors' model, which seems to work out quite well), I have found that scientifically it eventually "only" corroborates our existing understanding, at least mostly. I.e. it has remained unclear to me what aspects of the study ultimately contribute "new knowledge". The authors may in general want to better work out where such added value (to the community) exactly lies.

C1

Main comments:

A central topic of the Title, i.e. the role of precursor species in H2SO4 new-particle formation, seems not well represented in the introduction. I suggest better guidance here (in the intro) for the reader as to where the paper will be heading to (hopefully, presuming at this stage, to the role of precursor species). Indeed, it kind of remains unclear, at first, what is actually meant by 'precursor' (e.g. after reading the abstract). And the word 'precursor' actually only appears once in the entire text, referring (I believe) to involved in the reactions leading to the formation of H2SO4. But it hasn't been clear to me until quite a bit into reading the manuscript, if this was the (only) kind of 'precursor' the authors had in mind with the title. ... Finally, after reading the manuscript, I actually doubt that the title is appropriate, as I don't actually see the "dependence on precursor species" in both SA and particle production as a main topic of the work as a whole. Maybe that will change in a revised manuscript. But essentially, I am seeing a study of SA formation and subsequent particle formation, with most of the work going into explaining what drives particle formation and growth rates. It is certainly carefully carried out and explained (and almost throughout nice to read), but ends up mostly confirming the community's understanding of the underlying processes. 'Dependence on precursor species' is part of this, but I feel it is not the overall "new thing" here.

Fig. 2 would benefit from a discussion, better (if possible) display of, uncertainty estimates. E.g., the authors themselves mention large corrections applied in case of small particle sizes (section 3.1, 2nd paragraph).

C2

Style Definition: Normal: Indent: First line: 0.2"
Style Definition: Heading 1: Indent: First line: 0.2"
Style Definition: Heading 2: Indent: First line: 0.2"
Style Definition: Heading 3: Indent: First line: 0.2"
Style Definition: Heading 4: Indent: First line: 0.2"
Style Definition: Betreff: Indent: First line: 0.2"
Style Definition: Header: Indent: First line: 0.2"
Style Definition: Kontakt: Indent: First line: 0.2"
Style Definition: Name: Indent: First line: 0.2"
Style Definition: Copernicus_Word_template: Indent: First line: 0.2"
Style Definition: MS title: Indent: First line: 0.2"
Style Definition: List Paragraph: Indent: First line: 0.2"
Style Definition: Affiliation: Indent: First line: 0.2"
Style Definition: Balloon Text: Indent: First line: 0.2"
Style Definition: Equation: Indent: First line: 0.2"
Style Definition: Caption: English (U.S.), Indent: Left: 0.2", Right: 2.6"
Style Definition: Footer: Indent: First line: 0.2"
Style Definition: Correspondence: Indent: First line: 0.2"
Style Definition: Authors: Indent: First line: 0.2"
Style Definition: Comment Text: Indent: First line: 0.2"

Comment [R1]: We agree with this point and believe this reviewer detailed this issue in their comment at the bottom of C4 regarding a more systematic presentation of the results. Indeed ... [1]

Comment [R2]: We have a new title (see ... [2]

Comment [R3]: New title: "H2SO4 and p ... [3]

Comment [R4]: We added a paragraph or ... [4]

Page 6, line 5 & Fig. 2: Has the change in particle size distributions (PSD) between 2/23 and 5/15 (Fig. 2b) occurred gradually? With only those two chosen dates shown in Fig. 2b, one wonders how reproducible the PSD were overall, also considering substantial variations in 'baseline' total number concentrations (Fig. 2a).

Comment [R5]: We were prompted to examine more data and we finalized and thus added data to the paper: from mid-May through June 20. We therefore added several distributions to the former Fig. 2a, added a second figure for the new data and moved them both to the Supplement. The distributions do not show a clear secular trend outside the scatter. There are time periods with unique characteristics in N_p and D_{le} (in the new Fig. 2 a nd b) but we now state that, within the scatter, there is not a substantive change since the mesh was installed.

Fig. 4: The legend of panel (a) needs some explanation. The last sentence of the caption misses a verb or something.

Comment [R6]: Fig. 4a is moved to the Supplement and its caption was better explained.

Section 3.2.2 (varying SO2) First (page 9, line 5 & Fig. 5, I suggest to also show the model case excluding the HO2+SO2 reaction be in Fig. 5. That would quickly illustrate how model results improve and also make this paragraph easier to understand.

Comment [R7]: This is now done and there is a clear difference in the model runs. Note also that we updated the model to use thermodynamics better suited for 52% RH which greatly affects predictions for the binary system. See the next comment for more details.

Then, I am not sure I completely follow the matter of the NH3. 70 pptv of NH3 at inlet were assumed in the modeling (also lines in Fig. 5), but do I understand correctly that no NH3 was added for the experimental data shown, and NH3 is assumed as contaminant? Especially, as later in this section the potential role of ppq levels of dimethylamine is discussed, I'd be curious to see how the model would play out in the absence of any contaminant (i.e. also without NH3). That would maybe lead to the question: How much dimethylamine would be needed INSTEAD of NH3 to _fit the experimental data? Again, I might have run into a misunderstanding, in which case some clarification would benefit the section...

Comment [R8]: This comment prompted a hard look at this issue. (1) We realized that the 16 % RH thermodynamics we had used poorly represents the binary kinetics at 52 % RH. Thus a new set of H2SO4-H2O thermodynamics for 52 % RH was developed using the methodology outlined in Panta et al. 2012. A new section in the Supplement (S8) contains a description of this process and lists the new 52% RH and the (old) 16 % RH cluster free energies.

Comment [R9]: The binary (absence of contaminant) model results are significantly lower than the experimental work. We had pointed out in the previous version that 5 ppqv of dimethylamine gave the same Np as ~ 100 pptv ammonia, a finding now shown in Fig. 8. This figure goes with a new section in the paper **(3.3. Contaminants…** ; the current 3.3 will be renamed 3.4) that presents these comparisons in detail. This section will focus on characterizing the type and amount of possible contaminant in PhoFR.

Fig. 6: The legend of panel (b) needs some explanation. (Cf. comment on Fig. 4 above.) Same issue also in Figs. 9 and 10.

Comment [R10]: Fig. 6(a) was also moved to the Supplement and its caption was fixed. The Np information from the distributions in Figs. 9 and 10 are plotted in Fig. 4a and one distribution is plotted in Fig. 4b. Figs. 9 and 10 are included in the supplement (S3.2).

Comparing Figs. 6b and 4a, and as per the related discussions in section 3.2, it looks like the addition of NH3 makes the leading-edge mode easier to fit, as the <10-nm minimum is more pronounced. This is in agreement with the model simulations (Fig. S1). However, in Fig. 2b (and discussion), the less pronounced minimum had been

C3

attributed to more contaminants contributing to new-particle formation in the earlier (vs later) times of spring. (Actually, Fig. 2b vs. Fig. S1 is already discussed in section 3.1 also.) So from that, one could conclude at least that "contaminant" 6= NH3. But following the CLOUD works and others, it seems most likely however that NH3 or other base compounds (amines) would be the primar suspects as for the kind of contaminant suspected. So I see a contradiction here. To resolve that, I suggest the authors discuss somewhere, how purported contaminants would make that minimum (_2.4nm) less pronounced, whereas if bases ("contaminants") were added upstream the opposite would be observed. (And, if applicable, if effective contaminants to blame for Fig. 2b could be something other than bases.) Is it merely the different spatial distribution of contaminants vs. added bases in the flow tube? But if so, does the model manage to simulate those observations, and how does that align with my comment on (understanding of) section 3.2.2 above?

Comment [R11]: This was a temporal minimum as discussed above in R5.

Comment [R12]: We agree.

Comment [R13]: It is also the type of contaminant: added DMA at the top gives a differently shaped distribution than added NH3 at the top. We have greatly expanded the S1.3 Model results in the Supplement to show this. The new section 3.3 in the paper, discussed in R9 above, will discuss these issues.

Section 3.2.3, last paragraph: Is the DMA simulation (I assume it is simulation results) shown somewhere? What is "experiment base"? Not sure I understant that sentence. And maybe as a consequence, I am also not sure I understand the follow-up sentence (page 10, line 1). In any case, I think the sudden introduction of amides and some not-more-closely defined "strength" is confusing.

Section 3.2.6, DMA additions: It is stated that Np increases _linearly with [DMA]. Could be good to show, similarly to Fig. 8? (In the Supplement possibly.) Same for D_le. Actually, there is reference to a Np-vs-[SA] figure in the Supplement, but again it is very hard to find it.
Not sure how that would work out, but maybe there could be unified plots of N_p vs. [X] (and of D_le vs. [X]), i.e. showing all X in one figure. In general, the various effects of changing inputs on N_p and D_le are presented somewhat inconsistently. E.g., N_p vs [NH3] is shown (Fig. 7), but N_p vs [DMA] is not, neither is D_le vs [NH3] (whereas D_le vs [HONO] and D_le vs [RH] are shown). Another example is maybe Fig. S9 in the Supplement: It shows model results together with experimental data for some

C4

cases but not for others. I could imagine that the paper would benefit from a more systematic presentation of the various results.

Page 13, line 27 vs. line 10 & Fig. 11: First (and Fig. 11), it says that the H2SO4-power dependence here was close to those by Yu et al. and the findings from CLOUD. Then, a H2SO4-power dependence from CLOUD of 2.6 is mentioned to be somewhat lower than the one found here. Why this difference (apparent contradiction)?

Minor comments:
Page 2, paragraph starting at line 12: Instead of only listing the questions approached by the community in recent years, I think it would be more instructive to also shortly summarize the state-of-the-art in our ability to answer the listed questions.

Page 2, paragraph starting at line 18: Not clear, what levels of contaminant base compounds were (a) determined or estimated to have been present in the cited past studies vs. (b) suggested to have played a role in altering the outcome of the respective results.

Page 3, line 4: Though clarified later, I was confused here, if the results presented in the paper were all obtained with that Teflon screen in place, or only some? Anyway though, how was the "jetting" from the inlets manifest, so that it was decided to include the screen? In other words, why was it decided to put the mesh there?

Page 7, line 18: I am unfamiliar with the meaning of "truncated" here.

Fig. 5: Caption mentions orange lines, but plots are B&W.

Page 9, line 31: Please indicate more precisely where in the Supplement the information is. I couldn't actually find the place for certain.

Page 10, line 5: Don't see red squares in Fig. 7.

Page 10, line 8: Again, would prefer a more specific reference to where in the Supplement.

C5

Page 13 & Fig. 11: As the Sipila et al. (2010) results are discussed, it could be nice to present them also in some way in Fig. 11.

Comment [R14]: The DMA simulations are now presented in the new section 3.3 as well as the supplment. The variation with SO2 and contaminant as DMA was mostly speculative and the paragraph at the end of 3.2.2 was removed. The word base in 'experiment base' was removed.

Comment [R15]: With the new organization of the data, this section is now largely re-written. We do not emphasize any linearity in the exp. behavior of Np with DMA level (only three data points). The Supplement figure referred to here is now Fig. 8.

Comment [R16]: Figs. 4 and 6 have the data consolidated in such a manner. The D_le for the Fig 2a data is plotted in 2b just below the Np data. The consolidation within the paper and supplement we believe has led to a more systematic line of reasoning.

Comment [R17]: Line 10 was referring to the binary system and line 27 referred to the added ammonia cases. Yet this discussion was removed because it added little.

Comment [R18]: We have significantly re-worked this paragraph on p. 2, listing the state of the art information and categorizing the uncertainties in this paragraph as important but known and somewhat quantifiable

Comment [R19]: We reworded lines 20-30 on p. 2 to establish clarity.

Comment [R20]: Another reference to the date Feb. 23 has been added. There is an indicator in Fig. 2a at this date.

Comment [R21]: We did flow visualization experiments, as discussed in our much earlier work in Ball et al. (sentence added on p. 6.)

Comment [R22]: This word was not used in the revised text.

Comment [R23]: They were orange in a draft version, which we overlooked upon editing. Caption is fixed.

Comment [R24]: The 3 ppqv DMA data was erroneously listed here; should have been noted as 5 ppqv (Fig. S9). This text and figure (Fig. 8) are included in the new section "3.3 Characteristics of a potential contaminant" p. 13.

Comment [R25]: They are black in the submitted version (they were once red in a draft.) In the revised figure (Fig. 5) they will be red again. And the data at lower Q4 in Fig. 5 will be yellow.

Comment [R26]: This was Fig. S8 and it is now Fig. S6 which is referred to on p 11 line 7.

Comment [R27]: Yes, now included in Fig. 9.

Page 13, line 33 (and before/after): I can't quite follow these sentences, pitching the Glasoe et al. data against various other datasets (including the present one). Please clarify. To accompany the discussion of the effects of NH3, it may be illustrative to show a figure similar to Fig. 11 (i.e. comparison to literature results) but showing J-vs-[NH3].

Fig. 9 has two sets of data for DMA = 0 pptv (one denoted as "0", the other as "0.0" in the caption). Is there a difference or where these just repeats?

Fig. 11, including caption: Explanation of the dotted line and the marking "x^3.7" is missing. It would also be good to be more precise with the citations in the legend. (E.g., "Kurten, 292K" doesn't assure me I'll be ending up with the correct work if I decide to check it out.)

Fig. S5 misses a caption.

Fig. S9 as well.

Comment [R28]: We have greatly expanded the discussion of this issue. We have also now included such a figure, Fig. 10 along with a new section 3.4.1.

Comment [R29]: There were repeats: just before and just after DMA was added. These plots are now in the supplement (Fig. S3.2).

Comment [R30]: We have heavily re-worked Fig. 11 and its caption; it is now Fig. 9.

Comment [R31]: Added. Now it is called Fig. S3.1.2.

Comment [R32]: Captions are now added for former figures S8 and S9 that are now Figures S6 and Fig. 8 in the main paper, resp.

Interactive comment on Atmos. Chem. Phys. Discuss., https://doi.org/10.5194/acp-2018-1355, 2019. C6

Anonymous Referee #2

Received and published: 28 February 2019

The paper by Hanson et al. reports on measurements made with a photolytic flow reactor (PhoFR). The PhoFR is used for nucleation studies where new particle formation is initiated from reactions involving mainly sulfuric acid and water. Additional measurements were made by adding base molecules, i.e., either diluted ammonia or dimethylamine are added to the flow reactor. The sulfuric acid is generated from the photolysis of HONO and further reactions involving SO2, O2 and H2O. After a reaction time of approximately 30 s the particle size distribution is determined with a nano-differential mobility analyzer and a condensation particle counter using diethylene glycol. The measured size range covers diameters from approximately 2 nm to the largest sizes the particles can reach after the short reaction time, i.e., _10 nm. The particle number from integration of the size distribution is used to derive new particle formation rates. C1 With this information, the values from the present study are compared with other experiments and especially for the binary experiments (sulfuric acid and water); the data from the present study agree well with other data from the literature. For the ternary experiments involving ammonia, some discrepancy is reported. Further results are presented that show the variation of the integrated particle number and the particle size with the concentration for different gases. Results from a model involving various gas-phase reactions and the photolysis of HONO are shown for a comparison. Hanson et al. are also suggesting that a reaction between HO2 and SO2 could be relevant for forming sulfuric acid for the conditions of their flow tube experiment. I mainly agree with the conclusions drawn by the authors and the experimental data are mostly carefully evaluated and discussed. However, there is one major concern I am having regarding the experiments that involved ammonia (see below). After this point is addressed in a revised manuscript, I recommend publication in ACP.

(1) The bases (either ammonia or dimethylamine) are added from a sidearm into the flow reactor. The concern I am having is that this geometry does not ensure proper mixing and homogeneous distribution of the base. This possibility should be discussed and ideally, it should be evaluated in how far the mixing is homogeneous and if incomplete mixing could have influenced the results. For example, the results shown in Figure 7 suggest a relatively weak dependency of particle formation with the ammonia mixing ratio that is not consistent with other studies cited by the authors. Could this be related to the way the base is introduced into the flows? Another factor that can have an influence on the ammonia concentration is the mesh that is present in the flow reactor. It seems that the diluted NH3 needs to pass that mesh before it can contribute to new particle formation. Almost certainly, some of the ammonia will be lost on the surfaces of the mesh, especially since its surface is acidic (as it has been soaked in a dilute sulfuric acid solution). More discussion related to these questions is required in the revised manuscript.

Comment [R33]: We have added two sections in the Supplement (S3 and S7.1) explaining the findings from our previous publications on this topic and we present results from model simulations that mimic inhomogeneous mixing (Figures S7.1).

Comment [R34]: Yes, data are not consistent with calculations based on the thermodynamics derived from some of our previous data. One of our conclusions in this paper is that the Glasoe et al. ammonia data may have been affected by small amounts of amines that were carried in with the ammonia. For the present experiments, base was introduced in a similar manner as in Glasoe et al. but we were careful to not expose the ammonia dilution system tubing to any other base species.

Comment [R35]: We have clarified in the text and in Fig. 1 that the mesh is upstream of the base addition port.

Further comments:

C2

P4, L4: Please use the correct spelling for some of the references (e.g., Sipilä et al. but also others). In addition, the references should be checked; for some of them, the year is not correct in the list or has not been cited correctly in the text

P3, L8: µmol / mol ?

P3, L12: I think the word “additions” should be deleted

P4, L12: The year is missing here for the reference to Lovejoy et al.; this is the case also for other references in the main text

P5, L4: Does the outcome of the model depend on the flow setting? What mode is the “correct” one?

P5, L14: As can be seen from Fig. 1a the base is added from a sidearm at the end of the conical glass piece. Based on the geometry and the rather low flow rates it seems unlikely that the base is equally distributed over the whole cross section of the reactor. Has the possibility of inhomogeneous mixing been examined?

P5, L27: “. . . data were binned . . .”; please check the whole manuscript and use plural when using the word data

P6, L7: In the SI a detailed definition for the leading edge is provided; it would be good to provide a reference here to the SI regarding this exact definition

P7; L23: A definition for Z is missing

P8, L10 to L11: The process described here (scavenging of H2SO4 on the particles) is particle growth by condensation, which should be linear with the concentration of the condensing vapor (see, e.g., Nieminen, T., et al., 2010 ACP). Therefore, I do not understand this argument.

P9, L1: It would be good to include also curves from the model that do not include the HO2 + SO2 reaction in order to see the difference.

C3

P9, L6: ppmv instead of pptv?

P9, L12 to L16: I might have missed this but how exactly is the nucleation of particles modeled? The model needs to include evaporation rates for the smallest clusters. How are they obtained?

P9, L28 to L30: In this context, it should be noted that the factor of a 100 refers to the ratio of experiments with several hundred pptv and 4 pptv (which is the estimated contaminant level at 292 K in the Kürten et al. (2016, JGRA) study). For lower baseline (contaminant) NH3 the enhancement factor is very likely much larger.

P9, L32: Is the conclusion then that the contaminant ammonia level is _70 pptv for

Comment [R36]: We apologize for our poor attention to detail in our reference list. Many have been fixed and we discovered we had missed some in the list.

Comment [R37]: Yes.

Comment [R38]: Correct.

Comment [R39]: Done.

Comment [R40]: Good questions and a new section in the Supplement was added, S7.2. The modeled Np depends only slightly on which radial profile is selected. The distributions do change significantly between plug and laminar shown in S7.2. We also present evidence that the flow is expected to be fully developed laminar.

Comment [R41]: This issue is important (also brought up in R1) as it goes to how well the model can be compared to experiment. Our previous CFD work (Hanson et al. 2017) was a 3D model and thus could explicitly take mixing into account. In that work we also detailed the model used here (called 2D-LFR in that work) and presented an alternative way that base could be introduced in the model that would mimic - in part and maybe good enough - the inhomogeneity of the mixing. This mimic was to confine the base in the middle 1/4 of the mass flow. We add such simulations here and present them in the supplement (S7.1) with a reference to this section in the main text.

Comment [R42]: Thank you.

Comment [R43]: Will do.

Comment [R44]: We took out this text. It was replaced by text describing a similar point.

Comment [R45]: We no longer discuss the departure from linearity as it applies to only about 5 data points. Yet we want to clarify: we were arguing that as particle surface area grows, it begins to become a significant loss process compared to wall loss. So at large enough particle surface areas, no longer would H2SO4 be linear with HONO.

Comment [R46]: Done.

Comment [R47]: Correct.

Comment [R48]: The thermodynamics of the clusters largely determine their evaporation rates and they are included in the model. Please see Hanson et al. 2017. Note we also added a section in the Supplement with cluster free energies.

Comment [R49]: Lines 26 and 27 are very much in line with this assertion. We have added this suggestion as it is reasonable.

the set-up of the present study? This higher contaminant level (relative to the CLOUD experiment) could possibly explain the differences between the present and the Kirkby et al. (2011, Nature) study (Fig. 11).

P9, L33: Delete the word "base"
P10, L5: Replace "red squares" with "open squares"

P10, L10: The slope in Fig. 7 seems to be closer to 0.5 than to 1. How can this be explained?
P11, L24: Delete the word "and"
P13, L33-L34: This is one possibility; however, further discussion regarding the uncertainties of the present study is necessary. First, how would inhomogeneous mixing (of NH3) influence the outcome of the present study? Second, is it possible that NH3 is lost on the Teflon screen between the conical and the cylindrical glass pieces? It is mentioned that the screen was soaked in a dilute H2SO4 solution. Therefore, it could be that a significant fraction of NH3 was lost on the mesh, which could lead to lower Np in comparison to the previous studies (Glasoe et al., 2015 JGR and Hanson et al., 2017 JPhysChemA).

P22, Fig4, L4: Please include "the CPC" before "raw count rate"
P23, L4: "orange line", please check

SI:
P6, S5.2: The PTrMS is mentioned here. In terms of checking the homogeneity of NH3 in the flow through the reactor, this instrument could possibly be used to measure ammonia at the outlet of the reactor when the lights are off.

P7, L3 to L4: References are missing here and the last sentence is incomplete.

P7, end of section S5.2: It should be explained why exactly this is consistent with expectations.

P7, S6, end of first paragraph: It is mentioned here that Np increases with time for a set NH3. If this is the case, how are the results with ammonia exactly obtained? Were the data only evaluated after a long enough waiting time? How long was this period and did the Np level off eventually for all measurements?

Comment [R50]: The contaminant is consistent with 200 pptv NH3 (using new thermodynamics, NH3_52). This seems a rather high level to not be depleted by simple evaporation. And the simulations with DMA at ~0.005 pptv shows that gas-phase DMA gets depleted by clusters such that Np variations with HONO don't match experiment. So we consider other base species like methylamine (we were mistaken to suggest an amide) that is of intermediate strength in nucleation. We have adding a figure and discussion of the model simulations in a new section (3.3) in the paper.

Comment [R51]: Thank you.

Comment [R52]: We now have red and yellow open squares in the new figure.

Comment [R53]: The reviewer must have thought this was a log-log plot? The data were represented by a fitted line in that plot. But this plot is superseded by the new figure 5 which is a semi-log plot and includes more data. The whole discussion on the linearity of this data has changed.

Comment [R54]: Replaced with a comma.

Comment [R55]: Loss on the mesh is not an issue and inhomogenieties are now discussed in the Supplement FigS3.1 and S7.1 (see also R33, R35 and R41 above.)

Comment [R56]: No longer applicable in this plot but in the new Fig. S1 CPC was added.

Comment [R57]: Done.

Comment [R58]: Since ammonia is lost on the wall, very little makes it to the end of the tube. This was also the case for the Glasoe et al. experimental work. The model assumes diffusion limited loss to the wall and there is less than 1 % of the added ammonia that exits the flow reactor. More important, the model suggests that the diffusion-limited-wall-loss radial profile for ammonia is established after a length of about 15 cm.

Comment [R59]: These are fixed. Note: we re-confirmed the analysis and present equations to derive photolysis rates from the isoprene photoxidation results. There is no substantive change in the calculated photolysis rate.

Comment [R60]: True. This data is now shown in a separate plot (Fig. S5.2 right) and it was analyzed in the text as well.

Comment [R61]: An increase in Np with time was noticed only when 2000 pptv was added and it was particularly dramatic on the second consecutive day as can be seen in the figure (S6). For all the other base-added measurements, counts were generally stable after an initial surge in Np (e.g. 20 min) upon introduction of the base-addition tube into PhoFR. This initial surge can be seen in Fig. S1 in the new S1.0 section with raw data plotted vs. time.

P8, Table 1: The model does not seem to include the photolysis of NO2. This can lead to an increased NO concentration and in turn increase OH (from HO2 + NO). Photolysis of H2O2 can further enhance the OH level. When these reactions are implemented, is there still a need to include the HO2 + SO2 reaction? Furthermore, is the presence of HNO3 further considered? It could possibly also be taken up by the aerosols.

Interactive comment on Atmos. Chem. Phys. Discuss., https://doi.org/10.5194/acp-2018-1355, 2019.

Comment [R62]: We agree that this chemistry occurs but those reactions are negligible compared to the first-order photolysis of HONO and reaction of HO2 with NO. NO2 photolysis would occur but less than 10 % would be depleted over the course of the reactor. We tested this photolysis in the simulation and there was less than 1 % change in H2SO4. If we added NO2 coming in as an impurity, it acted to scavenge OH and decreased H2SO4. H2O2 photolysis at 350-380 nm would be extremely slow. HNO3 uptake is possible but would not explain any SO2 dependence for the total number of particles. The reactions suggested in this comment would not be affected by the level of SO2.

H_2SO_4 and particle production in a Photolytic Flow Reactor. Chemical modeling, cluster thermodynamics and contamination issues

David R. Hanson[1], Hussein Abdullahi[1], Seakh Menheer[1], Joaquin Vences[1], Michael R. Alves[1,2], and Joan Kunz[1]

[1] Chemistry Department, Augsburg University, Minneapolis, MN 55454, USA
[2] Chemistry and Biochemistry, University of California - San Diego, La Jolla, CA 92093, USA

Correspondence to: D. R. Hanson (hansondr@augsburg.edu)

Abstract. Size distributions of particles formed from sulfuric acid (H_2SO_4) and water vapor in a Photolytic Flow Reactor (PhoFR) were measured with a nano-particle mobility sizing system. Experiments with added ammonia and dimethylamine were also performed. $H_2SO_{4(g)}$ was synthesized from HONO, sulfur dioxide, and water vapor, initiating OH oxidation by HONO photolysis. Experiments were performed at 296 K over a range of sulfuric acid production levels and for 16 to 82 % relative humidity. Measured distributions generally had a large particle mode that was roughly log-normal; mean diameters ranged from 3 to 12 nm and widths (lnσ) were ~0.3. Particle formation conditions were stable over many months. Addition of single-digit pmol/mol mixing ratios of dimethylamine led to very large increases in particle number density. Particles produced with ammonia, even at 2000 pmol/mol, showed that NH_3 is a much less effective nucleator than dimethylamine. A two-dimensional simulation of particle formation in PhoFR is also presented that starts with gas-phase photolytic production of H_2SO_4 followed by kinetic formation of molecular clusters and their decomposition determined by their thermodynamics. Comparisons with model predictions of the experimental results dependency on HONO and water vapor concentrations yield phenomenological cluster thermodynamics and help delineate the effects of potential contaminants. The added-base simulations and experimental results provide support for previously published dimethylamine-H_2SO_4 cluster thermodynamics and provide a phenomenological set of ammonia-sulfuric acid thermodynamics.

1 Introduction

Particle formation in the atmosphere has long been studied (McMurry et al. 2005; Kulmala et al. 2004) to ascertain potential impacts on health (Nel 2005) and on climate processes(IPCC 2013). For example, nano-particles (characterized as < 10 nm in diameter) can have special health effects as their small size allows for efficient transport into lung tissue (Kreyling et al. 2006). They also influence climate by growing to sizes large enough to affect radiative forcing and the properties of clouds. Despite numerous and wide-ranging studies devoted to understanding new particle formation, mechanisms and nucleation rates applicable to many regions of the atmosphere remain uncertain.

Deleted: Photolytically-Generated Sulfuric Acid and Particle Formation: Dependence on Precursor Species¶

Deleted: For standard reactant flows and conditions,

Deleted: , 52

Deleted: , and a ~40 s residence time, the calculated concentration of H_2SO_4 peaked at $1.2x10^{10}$ cm^{-3}, measured particle mean diameter was ~6 nm and total number density was ~10^4 cm^{-3}.

Deleted: were influenced by molecular clusters at small sizes, less than or equal to 2 nm diameter, but were

Deleted: dominated by

Deleted: particles

Deleted: are

Deleted: with

Deleted: ranging up

Deleted: a relatively constant

Deleted: σ of

Deleted: Particle number density and their mean size depended on relative humidity, HONO concentration, illumination, and SO_2 level.

Deleted: Ammonia

Deleted: levels up to

Deleted: at producing particles.

Deleted: reveals

Deleted: scales with

Deleted: its level builds along the length of

Deleted: flow reactor. Experimentally, particle growth scaled with HONO, in accord with model-predicted H_2SO_4 levels. Additional comparison between experiment and model indicates that reaction of HO_2 with SO_2 could be a significant source of H_2SO_4 in this experiment. The

Deleted: on particle formation rates near room temperature are addressed and provide context in comparisons with previous experiments.

Deleted: but do not support previously published

Sulfuric acid-driven nucleation is a prime source of nanoparticles in the atmosphere (Kuang et al. 2012; Sipilä et al. 2010) thus it is the starting point for many laboratory studies. Previous work on particle nucleation in the binary (water-sulfuric acid) system (Kirkby et al. 2011; Ball et al. 1999; Zollner et al. 2012; Ehrhart et al. 2016; Yu et al. 2017) have concluded that binary nucleation can be significant at low temperatures such as at high latitudes and in the upper troposphere. The sulfuric acid/water binary system also serves as an important baseline diagnostic for comparing experimental results. Finally, nanoparticle growth by sulfuric acid and water vapors is of interest as well as uptake of oxidized organic compounds by acidic nanoparticles. Good knowledge of the formation and stability of binary nano-particles is needed to understand their subsequent growth via other compounds.

Previous laboratory studies of nucleation in the binary system diverge widely, especially for results taken at or near room-temperature, suggesting experimental details may significantly affect results. For example, does it matter if H_2SO_4 is provided by a bulk or a photolytic source? Does the type of photolytic precursor, O_3, H_2O_2, H_2O, etc, matter? (Sipilä et al. 2010; Berndt et al. 2008; Laaksonen et al. 2008). The CLOUD experimental results at 278 K and below (Kürten et al. 2016; Ehrhart et al. 2015) has alleviated some of these concerns yet room temperature results can provide more stringent tests due to a greater sensitivity to thermodynamics. Other issues include (i) limitations imposed by particle detector characteristics as well as cluster/particle wall losses (McMurry 1983; Kürten et al. 2015; 2018) and (ii) determining the concentration of H_2SO_4 (Sipilä et al. 2010; Kürten et al. 2012; Young et al. 2008) which is typically uncertain to a factor of two (Eisele and Tanner, 1993), although higher accuracies (±33%, Kürten et al. 2012) can be achieved. These experimental challenges can significantly influence results and their interpretation yet these largely known issues can be addressed to some degree.

Contaminants are the biggest unknown factor in these types of experiments and it is important to ascertain whether they are present at levels that can influence particle formation rates. If the contaminant is an amine, even a very low abundance can be a point of concern. For example, Zollner et al. (2012) argued that a 10^{-14} mixing ratio of methylamine could have affected their binary system measurements. Glasoe et al. (2015) presented data from the same apparatus as Zollner et al. and they carried this argument further and estimated that contaminant dimethylamine mixing ratios during their binary system measurements were less than or equal to 10^{-15}. If the contaminant is NH_3, however, it likely needs to reach the single-digit pmol/mol (pptv) level or higher to significantly interfere with measurements in the binary system at room temperature. Kirkby et al. (2011) and more recently Kürten et al. (2016) estimate ammonia contaminant levels of 4-to-10 pptv NH_3 for their experiments performed at 292 - 298 K; it is not clear if this level of ammonia had a significant effect on their results. Recently, Yu et al. (2017) reported upper limits for NH_3 and dimethylamine of 23 and 0.5 pptv, respectively, for their putative base-free nucleation experiments. Yet their nucleation rates are not extreme outliers, suggesting that their dimethylamine level was probably much lower than 0.5 pptv. Nonetheless, uncertainty introduced by undetectable (at the current state-of-the-art) levels of contaminants underscores the need for multiple approaches for studying sulfuric acid nucleation.

Deleted: Sipilae

Deleted: and

Deleted: or from which

Deleted: :

Deleted: . (Sipilae

Deleted: ? What are the

Deleted: 2015) ? How well-determined are the concentrations of H_2SO_4 (Sipilae et al. 2010; Jokinen et al. 2018) ?

Deleted: A prime concern

Deleted: contaminants

Deleted: abundances significant enough to

Deleted: ;

Deleted: (2015)

Deleted: Kurten

Deleted: .

Deleted: pmol/mol (

Deleted:),

Deleted: . Impurity

Deleted: this level would very likely overwhelm binary system nucleation which

Deleted: importance of assessing potential contaminants.

Here we describe an apparatus and results from experiments on the formation of sulfuric acid nanoparticles from photolytically-generated sulfuric acid vapor **via** OH+SO_2 photochemistry initiated with HONO photolysis at ~350-to-370 nm. Although nitrous acid is considered an important contributor to OH radical formation in many situations (Sörgel et al. 2011), little has been done to understand its photolysis that leads to sulfuric acid formation and new particle formation. We also studied the effects of adding ammonia or dimethylamine; both are known to greatly enhance particle production rates (Almeida et al. 2013; Glasoe et al. 2015; Yu **et al.** 2012; Ortega et al. 2012; Nadykto and Yu 2011). **We present experimental results where temporary contamination of** the **apparatus was evident yet long-term results indicate a relatively constant level of cleanliness in the experiment. The** experimental results are compared to simulations of the flow reactor that couple the flow with photo-chemical kinetics and an acid-base particle formation scheme. **In addition to providing H_2SO_4 concentrations, the model results and their comparison to experimental particle characteristics has led to phenomenological cluster free energies for the ammonia-sulfuric acid system at 52 % relative humidity. Finally, we present a compendium of results from photolytic particle formation experiments near room temperature.**

Deleted: (the

Deleted:).

Deleted: , McGraw, and Lee

Deleted: Finally,

2 Methods

The Photolytic Flow Reactor (PhoFR) is a vertically-aligned cylindrical glass tube with an inner diameter of 5.0 cm, a length of ~130 cm, a volume of approximately 2.5 L and topped with a 23 cm **long** conical glass piece with several flow inlets (Fig. 1a). In the course of this work, a Teflon screen was positioned between the cone and the flow reactor to calm the jetting from the inlets. A ~ 105 cm **length** of PhoFR is jacketed and kept at a constant temperature, typically 296 K, by circulation of thermostated water. The main flow of gas was nitrogen from a liquid nitrogen gas-pack and the total flow rate was 2.9 sLpm (standard L / min, 273 K and 1 atm). The flow contained small amounts of SO_2 and HONO, typically **16** and 0.02 µmol/mol (ppmv), respectively, and up to several % water vapor; relative humidity was set by sending a portion of the flow over a heated water reservoir and then through a thermostated, vertically-aligned tube that removed excess water vapor. Total pressure was slightly above ambient, ~ 0.98 atm: gauge pressure was monitored continuously and it was typically 0.001 atm. The oxygen level from the liquid nitrogen, stated to be 10 ppmv or less, was apparently sufficient for the subsequent oxidation chemistry - noting little differences in particle size **distributions upon adding several % O_2 to the flow. For all liquid nitrogen cylinder change-overs, the high pressure side of the regulator is flushed several times before exposing the lines to the new supply of gas - a standard procedure used by Ball et al., Zollner et al. and Glasoe et al. Also keeping in line with that past work, filters have not been used on any gas-supply lines.**

Deleted:

Deleted: portion

Deleted: a few

Formatted: Font: Symbol

Deleted: additions upon adding several % O_2 to the flow.

Entering gas flows were monitored and set by mass flow meters under computer control. Typical flows for baseline conditions in sLpm or sccm (standard cm^3 / min, 273 K, 1 atm) were dry gas at 1.4 sLpm, fully humidified air at 1.5 sLpm, HONO-laden (~15 ppmv) N_2 flow at 4.2 sccm, and SO_2-laden flow at 32 sccm (1500 ppmv SO_2-in-N_2). These baseline conditions help diagnose the long term stability of the system. The baseline number densities of SO_2 and HONO in the flow reactor (accounting for dynamic dilution) are $4x10^{14}$ and **$5.2x10^{11}$** cm^{-3}, respectively. **Three sections were not insulated or**

Deleted: , µmol/mol

Deleted: $6x10^{11}$

Deleted: The

thermo-regulated: (i) the conical top section**, (ii) the top 10 cm of the flow reactor where the base-addition port resides,** and **(iii)** the bottom 20 cm where aerosol was sampled**. The fully humidified line and the port where it enters the cone were gently heated (298-300 K) to eliminate condensation when room temperature was less than 296 K.**

The SO_2-in N_2 mixture (Minneapolis Oxygen) was reported (Liquid Technologies Corporation, EPA Protocol) to contain 1500 ppmv SO_2 +/- 10%. Water vapor was taken from a gently heated ~500 mL volume of deionized water (Millipore) that also contained a few grams of concentrated sulfuric acid to suppress potential base contamination from the bulk water. This humidified flow then passed through 80 cm of vertically-aligned Teflon tubing (~6.2 mm ID) held at the temperature of the flow reactor.

Photolyte HONO was continuously produced (Febo et al. 1995) by flowing nitrogen laden with ~15 ppmv HCl vapor into a small (25 mL) round-bottom flask containing 1-2 grams of powdered NaONO(s), held at 40-50°C (Fig. 1b). HONO vapor and co-product NaCl(s) are produced in a classic double-displacement reaction. The powder could be very slowly mixed with a small (1 cm long) stir bar and results generally did not depend on whether the powder was stirred. Periodic gentle shaking of the flask usually led to only temporary changes in particle number densities.

The HONO level exiting the generator is likely to be equal to the HCl level entering it. The HCl-generator and a water vapor pre-saturator were temperature-controlled at typically 20 °C. A saturated (~6 m, molal) NaCl aqueous solution in the pre-saturator yields a relative humidity of 76 % in the flow: a stable amount of water vapor stabilizes the solution in the HCl-generator, which contains a solution with a 2-to-1 mole ratio for NaCl to H_2SO_4. The HCl-generator solution was prepared initially with concentrations of 3.5 m NaCl and 1.75 m H_2SO_4 and calculations (Wexler and Clegg, 2002; Friese and Ebel, 2010) result in an HCl vapor pressure of 9.3×10^{-6} atm. UV absorption measurements to determine the HONO level in this flow are described in the Supplement **(S5.1)** and results indicate that the source has a HONO level of about 1.5×10^{-5} atm. This suggests that the HCl-generator's HCl vapor pressure is slightly larger than the calculated value. While the water vapor pre-saturator minimized loss of water from the HCl-generator, small temperature differences between these two vessels can introduce variability and possibly a bias.

Four black lights that have a UVA spectral irradiance centered at 360 nm illuminated about a 115 cm length of the jacketed flow reactor from a distance of about 15 cm from the reactor center. **An** estimate of the fluence (5×10^{15} **photon** cm^{-2} s^{-1}) indicates a photolysis rate **coefficient** of approximately 10^{-3} s^{-1} for HONO. Described in the Supplement **(S5.2) are experiments** where production of methylvinylketone and methacrolein from the oxidation of isoprene **were** monitored, yielding **(together** with the 15 ppmv HONO level **in** the **source flow) a** HONO photolysis rate **coefficient** of 8×10^{-4} s^{-1}.

H_2SO_4 is formed via (i) OH produced via HONO photolysis, (ii) OH addition to SO_2, (iii) H-atom abstraction by O_2 and (iv) reaction of SO_3 with H_2O molecules (Lovejoy et al**., 1996).** The HO_2 and NO radicals generated in this process can react together and generate an additional OH radical. When SO_2 is present at a few ppmv, the dominant loss for OH is OH + SO_2: a pseudo-first-order loss rate coefficient is given by $[SO_2]^* k_{OH+SO2} = 4 \times 10^{14}$ cm^{-3} * 8.9×10^{-13} $cm^3 s^{-1} = 360$ s^{-1}. With this SO_2 baseline level, OH reacts with HONO **for typical conditions** only about 1 % of the time: **the** OH first-order loss rate

Deleted: were not insulated or thermo-regulated.

Deleted: A rough

Deleted: photons

Deleted:

Deleted: is an experiment

Deleted: was

Deleted: an estimate (along

Deleted: discussed above) for

Deleted:

Deleted: .)

Deleted: an

coefficient is ~3 s^{-1}, from [HONO]*$k_{OH+HONO}$ = 5x10^{11} cm^{-3} * 6x10^{-12} cm^3s^{-1}. Yet at low SO_2 levels, loss of OH due to reaction with HONO can be significant.

H_2SO_4 levels build as the flow moves down the reactor, forming H_2SO_4 molecular clusters and these clusters grow into stable particles. These particles accumulate enough material, primarily H_2SO_4 and H_2O, to grow to several nm in diameter. Growth due to OH or HO_2 uptake followed by reaction with absorbed SO_2 may also contribute to growth.

Particles were sampled on axis at the exit of the flow reactor, about 120 cm from the conical inlet, with a custom-built mobility-sizing and counter system designed for nanometer-sized particles. Briefly, size-classified particles (Am-241 charger and a TSI 3085 nanoDMA) were detected with a diethyleneglycol (DEG), sheathed condensation particle counter (CPC) in tandem with a butanol-based CPC (Jiang et al. 2011). This system is denoted 'DEG system' in this study. The DEG CPC was operated with a saturator temperature of 57°C, a condenser temperature of 20°C, 0.36 L/min condenser flow and 0.07 L/min capillary flow. The nanoDMA was operated with 2 L/min aerosol-in and monodispersed-out flows and a 13 L/min sheath flow, as in Glasoe et al. (2015).

For a few experiments, ammonia or dimethylamine as trace gases were added through a port at the top of the flow reactor. A discussion of their mixing into the main flow is presented in the Supplement (S7.1). Their sources were permeation tubes, and 100s or single-digit pptv levels could be set by either a single- or a double-stage, respectively, dynamic dilution system (Freshour et al. 2014; Glasoe et al. 2015). Ammonia was used in the single-dilution system and dimethylamine was dedicated for use in the double-dilution system. Permeation rates were determined periodically by re-directing the base-laden flow through an acidic solution and monitoring the change in pH over time (Freshour et al., 2014).

2.1 Model

The 2-dimensional model of the flow reactor incorporating the photochemical kinetics of H_2SO_4 formation was built on a previous model of acid-base molecular cluster formation which was fully corroborated against a commercial computational fluid dynamics simulation (Hanson et al. 2017). The flow profile can be set to either plug or fully-developed laminar, the formation of clusters with up to ten H_2SO_4 and ten base molecules can be simulated. If so desired, clusters larger than ten H_2SO_4 molecules can be simulated using a growth-only mechanism. Note that clusters without a base molecule represent a weighted average of the binary H_2SO_4-H_2O thermodynamics for a given relative humidity. The detailed photochemistry in our experiment includes the production of OH, its reactions with SO_2 as well as with HO_2, NO, NO_2, HONO, HNO_3, H_2O_2 etc. The rate coefficients and mechanisms are presented in the Supplement (S7, Table S1). The acid and base species and all molecular clusters as well as OH are lost to the walls limited only by diffusion.

The model reacts, convects and diffuses all reactants and products and yields the abundance of H_2SO_4 and its molecular clusters, the largest clusters are then correlated to the abundance of experimentally determined particles (Panta et al. 2012; Hanson et al. 2017). Coagulation was not implemented, because cluster-cluster interactions are not significant for most of the conditions of the present work. Water molecules are not explicitly tracked but hydration is taken into when calculating the collisional rate coefficient and the size of the clusters, assuming bulk properties. Increases in

Deleted: For
Deleted: and
Deleted: systems
Deleted: 2D model here incorporates the
Deleted: , from
Deleted: through
Deleted: on
Deleted: is only crudely
Deleted: but these
Deleted: Also, the largest clusters can be grown to very large sizes via uptake of H_2SO_4 (and H_2O) assuming no loss.

computational times can be significant when large clusters are simulated using the growth-only mode, e.g. a factor of eight for adding clusters up to 250 H_2SO_4 molecules compared to stopping growth at the 10 acid, 3 base cluster. Yet it is desirable to simulate very large clusters via uptake of H_2SO_4 assuming no loss to compare results to measured size distributions. Further analysis of cluster growth and loss processes, including growth-only for clusters larger than 10 H_2SO_4 molecules, is presented in the Supplement **(S1.3).**

Ammonia or dimethyl amine could be included at a trace level with the flow entering the simulated reactor whereupon acid-base clustering and particle formation **commence** (note that base is lost to the wall, limited by diffusion). **The model assumes rapid mixing of base into the main flow. Justification for this is presented in the Supplement (S7.1).** The photochemistry is described in detail in the Supplement **(S7)** and the acid-base clustering reactions are described in detail in Hanson et al. **(**2017**)** along with thermodynamic schemes for clusters of the bases with sulfuric acid. **Scheme** DMA_I from that work **was used here while a new cluster thermodynamics scheme for the ammonia-added experiments was developed for NH_3-H_2SO_4 clusters at 52 % relative humidity (see S8).**

3 Results and Discussion

3.1 Particle formation evaluation.

The stability of particle formation conditions over several months is demonstrated by presenting the number and the average size of particles for baseline conditions. In the next section, the modeled photochemistry for baseline conditions is presented to provide baseline **sulfuric acid concentrations** within PhoFR**, and** we discuss how the size distributions were analyzed. In subsequent sections, these analytical devices will be applied to the results of experiments where reactant levels were varied. **In the Supplement (S1.0) is a typical time series of the raw data (the count rates for each channel) and a table with the overall correction factors.**

Shown in Figure 2 are **(a) the total particle number density, N_p, and (b) so-called "leading-edge" (see S1.1 in the Supplement) mode diameters** over a **6** month period for baseline conditions: 52 % relative humidity (RH), 296 K, total flow of 2.9 sLpm, and a flow of N_2 through the HONO source, Q_4, of 4.2 sccm. The data **were** binned according to the flow of the SO_2 mixture, Q_1, either 4 sccm or > **16** sccm. The abundance of HONO is 20 ppbv and SO_2 is either 2 ppmv or > **8** ppmv. **Shown in** the **Supplement (S1.2) are** representative particle size distributions - corrected for size-dependent diffusion losses in CPC transport and inlet lines. N_p was determined by summing the particle concentrations with D_p of ~2.4 nm and larger**, because the** two smallest diameter concentrations are **the local minimum for most of the size distributions. Furthermore, these small diameter data can** have large **random** uncertainties due to large corrections applied to low count rates**. Discussed in the Supplement (S4) are possible sources** of **the scatter in the data.**

Note the data presented as gold diamonds: these are N_p (low SO_2) on the day of, and the day after, a gas supply cylinder change-over. This event could be due to entrainment of dust particles into the supply lines. Nothing like this happened on the five other cylinder change-overs that occurred during this time interval. What is **different about**

Deleted: .

Deleted: commences

Deleted: thus

Deleted: also

Deleted: (those used here are primarily the NH3_I and

Deleted: schemes

Deleted: .)

Deleted: particle formation conditions

Deleted: . Here,

Deleted: also

Deleted:

Deleted: results

Deleted: 4

Deleted: was

Deleted: 20

Deleted: 10

Deleted: Fig. 2a shows

Deleted: total particle number density, N_p, and Fig. 2b shows

Deleted: . The

Deleted: not included because they

Deleted: ; furthermore, a mobility diameter

Deleted: 2.4 nm

this cylinder exchange is not known. The effects are temporary as a 90 % decrease in N_p occurred in a few hours, an additional 70 % drop occurred overnight and a day later N_p is within the upper range of the scatter for **baseline conditions.**

The measured size distributions are governed by the interplay between the spatial distribution of $[H_2SO_4]$, whether base is added, and the nature of potential contaminant species. For example, small- and **mid**-sized particles probably **form somewhat downstream** of the **top of the reactor whereas the** largest particles **at** the leading **edge** of the distributions are **formed near the top of the reactor.** The largest particles must originate at the top of the reactor, having the highest overall exposure to H_2SO_4. These so-called leading-edge particles are the focus of our analysis.

The leading-edge particles are greatly enhanced when base was added, whether ammonia or dimethylamine. In these cases, the leading-edge particles are prominent in the distributions and are described by log-normals (see the distributions presented below). The leading-edge volume-mean diameters for the added-base experiments are similar to those of the no-added base distributions. So we propose that the leading-edge particles are indicative of the nucleation conditions at the top of PhoFR. In the Supplement **(S1.1)** is more discussion of the leading-edge mode of the particle size distributions **and supporting results from the simulation (S1.2:** plots of modeled distributions **with and without added NH_3.)**

The high SO_2 data (Fig. 2a) exhibits an N_p that averages about $2x10^4$ cm^{-3} since late February; also the leading edge of the size distributions (Fig. 2b), fit to log-normal functions, indicate mode diameters of about 6 nm with $\ln\sigma$ values of ~0.35. The large drop in N_p on the 23rd of February is due to a Teflon mesh (ultrasonically cleaned and soaked overnight in a dilute sulfuric acid solution) placed between the cone and the flow reactor. The **edges of the Teflon** mesh **fit in the gap of the glass joint without disturbing the Teflon-encapsulated o-ring. The mesh was installed because flow visualization experiments, similar to those described in Ball et al. (1999), revealed extensive back-streaming into the cone. Back-streaming can carry H_2SO_4** from the illuminated section **into the cone to initiate** nucleation **there. With the Teflon mesh in place**, a trend in N_p **with time cannot** be discerned in Fig. 2a**. Similarly, leading-edge** mode diameters indicate that D_{le} is roughly constant **over the time period Feb 24 to Jun 20 (Fig. 2b).**

While the effects on N_p (Fig. 2a) due to the addition of the mesh are large, the effects on mode diameter are less pronounced. On the other hand, there is a five week period beginning the middle of April 2018 that has mode diameters about 1 nm larger than those during the preceding and following time periods. What was different about this time period is not known however potential changes in flow patterns and variations in room temperature are potential explanations.

Since changes in D_{le} are small or negligible, the growth conditions in PhoFR must be stable during this **5**-month time period. The cumulative exposure of particles to H_2SO_4 as they travel down PhoFR is constant, indicating that the UV flux and reactant concentrations are also. The **overall stability** in **N_p** during this time **also** indicates **that** the purity of the system **is stable. Variations in N_p might have been influenced by changes in potential contaminants, yet** the **HCl source for the HONO generator is temperature-sensitive and flow patterns can be influenced by temperature variations of the**

Deleted: local minimum

Deleted: most of the size distributions.

Deleted: the

Deleted: the middle

Deleted: decrease considerably between Feb. 23rd and May 15th (Fig. 2b) which is

Deleted: due to a decrease in particle-enhancing contaminants. Yet the concentrations

Deleted: are comparable in these two data sets: in other words,

Deleted: edges

Deleted: similar.

Deleted: ,

Deleted: and experimental leading-edge mode diameters (D_{le}) over time.

Deleted: limits backstreams

Deleted: that may introduce H_2SO_4 and thus

Deleted: in the cone. Ever since this big drop in N_p

Deleted: that is consistent with the changes with time of the size distributions in

Moved down [1]: Fig.

Deleted: can

Deleted: 2b. On the other hand,

Deleted: (presented in the Supplement)

Deleted: from January to May.

Deleted: 4

Deleted: decrease

Deleted: large particle numbers

Deleted: likely

Deleted: an increase in

Deleted: , for example a decrease in contaminant base levels entering

non-thermoregulated sections of the flow reactor. An expected increase in cleanliness over time, due to acid building up on surfaces and binding potential base-emitting contaminants, is not exhibited in the data.

3.1.1 Simulated reactant distributions

Shown in Fig. 3 are simulated centerline concentrations of the gas-phase species and two molecular clusters. In order of abundance at the end of the reactor on the left axis: H_2SO_4, NO_2, NO, HO_2, H_2O_2, HO_2NO_2 and NH_3; and on the right axis, OH, $(H_2SO_4)_2$ and 10^3 times the $(H_2SO_4)_{10}$ cluster abundance. This simulation was performed with [HONO] = $5.2x10^{11}$ cm^{-3}, simulating an experiment with Q_4 = 4.2 sccm. These conditions are close to those for the data depicted in Fig. 2 with the simulation being strictly binary nucleation.

Sulfuric acid rises steadily and reaches $1.2x10^{10}$ cm^{-3} by the end of the lighted section that extends from 0 to 110 cm. The downstream section of the reactor with the highest sulfuric acid level is where particles achieve most of their growth: over the bottom 2/3 of PhoFR, an axial distance of 40 to 125 cm, [H_2SO_4] averages about $8x10^9$ cm^{-3}. We partition the reactor into a top third and a bottom two thirds. Although somewhat arbitrary, it provides a point of view for discussing the experimental results. Furthermore, this point of view is congruent with the experimental finding that a large particle mode at the leading edge of the size distributions is discernible, especially so when base was added. So although clusters are formed and particles are nucleated along the length of the reactor, we seek to explain only the largest of them.

With this perspective, we can calculate from bulk properties the growth of the leading-edge particles due to their accumulating H_2SO_4 and H_2O (assuming no evaporation) as they traverse the bottom 2/3 of the flow reactor. Using centerline values, an increase in particle diameter of 4.8 nm is estimated as they travel from 40 to 125 cm, using the bulk approximation to calculate the increase in diameter (Verheggen and Mozurkewich, 2002; Wexler and Clegg, 2002). This is in accord with the leading-edge mode diameters in Fig. 2b of about 6 nm, considering that nascent particles are roughly 1.3 nm in diameter; using bulk properties for the 4 acid cluster assuming it is large enough for evaporation to be negligible. There is also a 0.3 nm difference between mobility and volume/mass diameters (Larriba et al. 2010). Thus modeled H_2SO_4 on-axis concentrations and residence time along with the assumption of bulk properties for the small particles is an adequate starting point for discussing growth in this experiment.

Growth was also explored with the model and simulated particle size distributions (Supplement, S1.3. Fig. S7.1) are consistent with the growth calculation in the preceding paragraph. The simulated clusters were grown to hundreds of H_2SO_4 molecules using growth-only for clusters larger than 10 H_2SO_4 molecules. The ammonia-added simulations show a D_{le} of about 4 nm (Fig. S1.3.1b) and 6 nm (Fig. S7.1) for Q_4 = 2.1 and 4.2 sccm, respectively. These mode diameters are consistent with the bulk-properties growth analysis.

The added-base simulations also provide information on nucleation near the top of the reactor. The axial distribution of critical clusters, assumed to contain 4 H_2SO_4 molecules, and those just larger reach a steady state by about 40 cm (Fig. S1.3.2) while very few of the 20 and larger H_2SO_4 clusters have yet formed. Nucleation in the top

Deleted: the
Deleted: of the system could also be
Deleted: buildup
Deleted: , potentially
Deleted: . The changes in the distributions over 2.5 months (Fig.2b) are due to decreases in particles
Deleted: middle of the distribution. Based on their size, these particles were nucleated downstream of where the leading edge particles are. The flow reactor wall may accumulate enough acid that may tie up a purported contaminant responsible for the mid-sized particles.
Deleted: the results of a simulation using the 2D model that shows
Deleted: : On
Deleted: ,
Deleted: $_2NH_3$
Deleted: 100
Deleted: SA_8
Deleted: $5x10^{11}$
Deleted: size distributions
Deleted: 2b.
Deleted: NH_3 was introduced at the inlet at ... [5]
Deleted: effect of added base on particle fo ... [6]
Deleted: despite the lowest sulfuric acid ... [7]
Deleted: levels
Deleted: ¶ ... [8]
Deleted: is
Deleted: but
Deleted: estimate
Deleted: Modeled particles that contain up ... [9]
Deleted: The behavior of
Moved (insertion) [1]
Deleted: truncated
Deleted: shown in Fig. 3 provides some ... [10]
Deleted: partitioning the reactor into
Deleted: top 1/
Deleted: a bottom
Deleted: /3. The abundance of $(H_2SO_4)_2N$ ... [11]
Deleted: involving base has reached its pe ... [12]
Deleted: Its behavior in the middle of

third of the flow reactor is important and heavily influences the large particle mode when base is present. Downstream regions contribute mid-sized particles that influence the shape of the simulated particle size distributions; this can be seen in binary, added-dimethylamine and added-ammonia simulations that are compared in Figs. S1.3.1c. Nonetheless, these simulations support a partitioning of the reactor **as a** rhetorical tool for discussing the results and for drawing broad conclusions **about the presence of contaminants in this region.**

3.2 Variation of N_p with [reactant]

3.2.1 Dependence on HONO

Shown in Fig. **4a are N_p vs. Q_4, the flow through the HONO source while the other reactants were held constant: 296 K, 52 % RH, SO_2 at 8 ppmv or higher. The data are primarily measurements without added base (black squares) but the results from two runs where base was added are also shown.** Fig. **4b are typical size distributions for measurements at Q_4 = 4.2 sccm for experiments with and without added base. Several more** representative size distributions as a function of **Q_4 are shown in the Supplement (S1.2).**

The N_2 flow through the HONO source, Q_4, **is** a proxy for HONO abundance **and thus sulfuric acid. The variation** of the volume-mean diameter of the leading **edge mode with Q_4 is presented in the Supplement (Fig. S1.2.2) and particle size scales approximately linearly with Q_4. This suggests that particles are exposed to linearly increasing amounts of H_2SO_4 over this range of Q_4. This data supports the Q_4-as-proxy notion that H_2SO_4 levels are proportional to the HONO concentration in PhoFR which is set by the nitrogen flow (Q_4) through the HONO source.**

The nominally binary N_p has a power-dependence on Q_4 of about 4 **(dashed line) which is also the case for the NH_3 added (230 pptv) data. For ammonia added at this level there is only a modest effect on N_p, a qualitative finding that is not congruent with recent experimental work (Kürten et al. 2016; Glasoe et al.** 2015). **For added dimethylamine at ~ 2 pptv, however, there is a large effect on N_p and on its dependence on Q_4, consistent with other experimental work (e.g. Glasoe et al.;** Almeida et al. **2013). More results and discussion of the added-base experiments are presented below.**

A power dependence of 5 for N_p on H_2SO_4 was exhibited for the H_2SO_4-H_2O binary system (Zollner et al. 2012) which is somewhat larger than that exhibited in Fig. 4b; other bulk experiments have power dependencies on H_2SO_4 that range up to ~20 (Wyslouzil et al. 1991; Viisanen et al. 1997). Yet the CLOUD experiment (**Kürten** et al. 2016), also with photolytic generation of H_2SO_4, shows a power dependency of 3.7 at 292 K for [H_2SO_4] concentrations from $3x10^8$ to $1.5x10^9$ cm^{-3}. An ammonia-contaminant abundance of 4 pptv was stated to apply to those results. Experimental results (Glasoe et al. **2015; Almeida et al. 2013) indicate power dependencies on H_2SO_4 are significantly affected when a base is present, corraborating the assertion that our nominally pure results were affected by the presence of an impurity base compound.**

Deleted: , a lag in its abundance profile compared to the SA_2NH_3 cluster, indicates that some catching up is needed to grow the clusters to 8 SA molecules. The increase in the abundance of these clusters with Z reaches a maximum near 60 cm. This indicates that the partitioning is a decent

Deleted: .

Deleted: , Dp

Formatted: Font: Bold, Subscript

Deleted: Variation of

Deleted: with no added base.

Moved (insertion) [2]

Moved (insertion) [3]

Deleted: Depicted in Fig. 4a are

Deleted: particle

Deleted: . Q_4 was varied from 1.6 to 5.3 sccm while the abundances of the other reactants were held constant. The size distributions are strongly dependent on HONO over this range, with concentrations increasing by a factor of ~ten at small sizes and the large particle abundance by a hundred-fold. Log-normal distributions are also shown as the dashed lines in the figure with leading-edge mode diameter D_{le} and $ln\sigma$ noted in the legend. The log-normals shown in the figure were not those from the fitting procedure (see the Supplement for more discussion of the fitting procedure) because two

Deleted: fits failed. For a consistent presentation, $ln\sigma$ was fixed and each log-normal was adjusted visually to best cover the four or five points nearest the peak of each distribution. N_p (Fig. 4b) and the

Deleted: edge mode, $D_{V,le}$ (Fig. 4c) are plotted vs. Q_4 and

Moved (insertion) [4]

Moved (insertion) [5]

Deleted: while $D_{V,le}$ increases linearly over most of this range.¶
It is reasonable to assume that the HONO concentration in PhoFR is linearly proportional to Q_4, the nitrogen flow through the HONO source. The data in Fig. 4c shows that $D_{V,le}$ scales approximately linearly with Q_4 up to about 7 sccm, suggesting that particles exposure to H_2SO_4 is also linear over this range. The departure from linearity is noticeable in

Moved up [3]: Fig.

Deleted: 4c and is probably affected by the inability of the fitting process (see Supplem ... [13]

Deleted: Kurten

Moved (insertion) [6]

3.2.2 Effects of added ammonia and dimethylamine.

When base was added to PhoFR, its mixing ratio was calculated assuming it has fully mixed and there is no loss to the wall. There is wall loss in the experiment and mixing of the base into the main flow takes an amount of time. Nonetheless, these mixing ratios are convenient for discussion and they are directly linked to the flow of added base. Care needs to be taken using these mixing ratios when comparing the results with simulations and other experiments. See the Supplement (S3.1 and S7.1) for more on base mixing into the flow.

With data for nominally clean conditions for comparison, the effect of 230 pptv NH_3 on the large particle abundance is significant in Fig. 4a, about a factor of 5, a factor that does not significantly depend on the level of HONO and thus H_2SO_4 present in the flow reactor. The experimental size distributions (e.g. red triangles in Fig. 4b) reveal a more distinct and larger leading edge mode than the nominally pure data. Plots of D_{le} as HONO was varied are presented in the Supplement (S3.1) and the effect of added NH_3 is a ~20% increase in D_{le}. The shift in the distributions to slightly larger sizes is due to enhanced particle formation in the top third of the flow reactor, shifting upstream the peak nucleation rates compared to that in the absence of added NH_3. This is supported by the simulated size distributions shown in the Supplement (S1.3) where the leading-edge of the size distributions becomes more distinct when ammonia is added to the simulations (Figs. S1.3.1).

Previous work has shown large increases in N_p when ammonia was added to a (nominally clean) binary sulfuric acid-water nucleating system. At H_2SO_4 concentrations of a few times 10^9 cm^{-3}, Ball et al. (1999), Zollner et al. (2012), and Glasoe et al. (2015) observed factors of 10-to-1000, ~1000, and 10^6 for ammonia levels of a few pptv, 25 pptv, and 55 pptv, respectively. Also, Kürten et al. (2016) showed that particle production in the CLOUD experiment increased by about a factor of 100 upon addition of several hundred pptv NH_3 at 292 K and $[H_2SO_4]$ of 1.5-2.2x10^8 cm^{-3}; this factor may have been even larger if the nominally binary system was not affected by a purported 4 pptv ammonia contaminant. We think that the presence of a contaminant in our nominally pure measurements is responsible for the low enhancement factors in particle numbers when 100s of pptv NH_3 are added. There will be more discussion on this below.

Dimethylamine addition at 2 pptv (+100/-50%) had a large effect on the number of particles (blue circles, Fig. 4a) and even the smallest particles (mobility diameter of 1.7 nm) increased by about 2 orders of magnitude (Fig. 4b). Nonetheless, the leading edge of the distributions is clearly the dominant mode for these conditions. It is interesting that the shape of the distributions is similar to the nominally binary cases (black diamonds, Fig. 4b). The Supplement (S3.2) presents additional measured size distributions for the dimethylamine-added experiments.

It is notable that N_p is not particularly sensitive to H_2SO_4 above Q_4 = 2.7 sccm. Model results also indicate a leveling off in the calculated N_p as Q_4 increases (see section 3.3 below) which appears to be due to scavenging of the

Moved up [6]: Experimental results (Glasoe et al.

Moved down [7]: SO_2. ¶
Particle size and number density were found to depend on SO_2 abundance. Shown in

Deleted: 2015;

Moved up [5]: Almeida et al.

Deleted: 2013) show that power dependencies on H_2SO_4 are affected when a base is present. The presence of an impurity base compound probably affected our experimental results. It may be due to two sources: (i) contaminant entering with the flows and (ii) contaminant emanating from internal surfaces. The added base experiments have more discussion on this topic but we note here that our system is slowly cleaning up over time. ¶
Particles grow due to uptake of H_2SO_4 and H_2O: the estimate from the H_2SO_4 profile from the model simulation discussed above suggests an increase in diameter of about 4.8 nm for a Q_4 of 4.0 sccm. The data in Fig. 4c show that the volume mean diameter is about 6 nm at this HONO level, which is consistent with that estimate. The agreement improves considering that nascent particles must attain a certain size to become stable, roughly 1.3 nm diameter or larger (large enough such that evaporation becomes negligible). There is a ... [14]

Deleted: Figs. 5 (a) and (b) are plots of N_p and $D_{V,le}$ (volume mean diameter of the leading- ... [15]

Moved down [8]: the flow rate of the SO_2 mixture, Q_1. HONO source flow rate Q_4 wa ... [16]

Deleted: : both increase with $[SO_2]$ and begin to level-off at high $[SO_2]$. This behavior is exp ... [17]

Moved down [9]: The experimental results show increases with SO_2 that are roughly in ... [18]

Deleted: Without a reaction between HO_2 and SO_2, the model shows small increases in N_p (40 % ... [19]

Moved down [10]: ¶ ... [20]

Deleted: There are disagreements in

Moved down [11]: whether HO_2 reacts with SO_2 as well as potential end products (Chen ... [21]

Deleted: Published

Moved down [12]: values for this rate coefficient range from upper limits of 1x10^{-18} ... [22]

Deleted: while leaving N_p undisturbed. ¶ ... [23]

Moved up [2]: Shown in Fig.

Deleted: 6 is the number of large particles vs. HONO flow rate taken with and without NH ... [24]

Deleted: nominal…ominally clean conditions for comparison, the effect of 230 pptv NH_3 on t ... [25]

Deleted: For example…t H_2SO_4 concentrations of a few times 10^9 cm^{-3}, Ball et al. (1999), Zoll ... [26]

amine by particles. Nonetheless, it appears that the potential contaminant for the nominally binary experiments is a much less effective nucleator than dimethylamine is at a level of 2 pptv.

Since effects due to adding dimethylamine at the single-digit pptv level are large, it would be desirable to experimentally investigate amine additions at lower levels. **With the current dynamic dilution system, base addition at levels lower than a few pptv are swamped by the precision uncertainty in the flow meter readings.** More results from these types of experiments await further improvement in the dimethylamine delivery system. **Another alternative is exploring conditions where nucleation is expected to slow such as at low Q_4 and/or at temperatures warmer than 296 K.**

3.2.2.1 Variation of N_p with added base.

Shown in **Fig. 5** are the total number of particles plotted as a function of added **ammonia level** for a fixed amount of HONO, **either** Q_4 = 2.1 **(yellow) or** 4.2 **(red)** sccm. The **open** squares represent the range of data obtained **for nominally binary conditions (**without added base**).** There are **significant** effects on N_p due to the addition of NH_3 at the top of the reactor, **over** a factor of ten for both sets of data.

At **large** NH_3 **exposures (**high levels **and/**or prolonged **addition) particle counts increased dramatically with** exposure **time, indicating a conditioning of the flow reactor wall.** This is demonstrated in the Supplement **(S6) that presents** measurements on days when 2000 pptv NH_3 was added. **The 2000 pptv NH_3 data in Fig. 5 were taken soon after ammonia introduction, minimizing the effects of high ammonia exposure.**

The large variability **of the NH_3 data** in **Fig. 5** mirrors the underlying variability in N_p without added NH_3 **(Fig. 4a)**. Yet, within the scatter of the measurements the dependence of N_p upon NH_3 **is** smaller **than** the 1.6 power dependence found in the bulk-source experiments of Glasoe et al. (2015). A **close to** linear dependence **on ammonia can be ascertained from the results of** other photolytic H_2SO_4 production experiments**;** the flow reactor experiments of Benson et al. (**2009,** 2011) and Berndt et al. (2010), and the 292 K CLOUD chamber experimental results (**Kürten** et al. 2016; Kirkby et al. 2011). **On the other hand, the 292 K ACDC theoretical ammonia-sulfuric acid nucleation rates predict a power dependence on ammonia of between 2 and 3, depending on conditions (Kürten et al. 2016).**

Simulated N_p as a function of added ammonia is shown in Fig. 5 and they are roughly in accord with the experimental data. The major discrepancy is at low added NH_3 where simulated N_p is significantly lower than experimental N_p. The presence of a contaminant that influences the experimental N_p, particularly at low ammonia levels, can contribute to this discrepancy. At high NH_3 levels, the effect of the contaminant was assumed to be diminished and the cluster thermodynamics were adjusted so that simulations matched experiment. Thus the experimental data at Q_4 = 4.2 sccm with ammonia ≥ 500 pptv guided the development of the H_2SO_4-NH_3 cluster thermodynamics used in these simulations (see the Supplement S8). We do not seek to establish the accuracy of the cluster thermodynamics but instead a phenomenological description of the results: the NH_3-H_2SO_4 thermodynamics developed and used here are phenomenological.

Moved (insertion) [13]

Moved (insertion) [14]

Deleted: Simulations are shown in the Supplement with two different NH_3 levels (70 and 300 pptv) that mimicked the Np vs. Q_4 data remarkably well (70 pptv NH_3 for the no-added base and 300 for the added base case). Dimethylamine levels at 0.003 pptv yielded N_p in the range of the experiment base suggesting that very small amounts of a contaminant can influence binary nucleation experiments. An amide may be consistent with the experiment: it is intermediate in strength (Glasoe et al. 2015), stronger than ammonia but not so strong that scavenging could be a major loss process. ¶ 3.2.4

Deleted: **NH_3 level.**

Deleted: Figs. 7

Deleted: NH_3 levels

Deleted: : (a) Q_4 = 4.3 sccm and (b)

Deleted: red

Deleted: at nominally zero NH_3

Deleted: .

Deleted: large

Deleted: up to

Deleted: NH_3

Deleted: (

Deleted:) particles counts rose dramatically.

Deleted: with

Deleted: Figs. 7

Deleted: Figs. 4b and 5a

Deleted: can be approximated as linear. This is a

Deleted: dependence

Deleted: is similar to

Deleted: ,

Deleted: Kuerten

Deleted: Simulated N_p are shown in Fig. 7a for two different thermodynamic schemes (Hanson et al., 2017); both clearly indicate a stronger dependence on

Deleted: than is exhibited in

Incomplete agreement across the **full range of** the **present** experimental results can **also** be due in part to **an inadequate** representation of the actual flow **and the mixing of base into the flow** in the simulations, however**, this would not be expected to depend on the amount of added-ammonia or on Q_4 (see Supplement S7.1 for more on base mixing into the flow.) Small changes to a few cluster free energies, 1 or 2 kcal/mol, can significantly alter predicted N_p.**

For ammonia levels greater than a few hundred pptv, this set of thermodynamics (labeled NH3_52) yields simulated N_p that varies with NH_3 to the 1.6 power for Q_4= 4.2 sccm conditions and NH_3 to the 1.9 power for the Q_4=2.1 sccm conditions. Since the dependencies on NH_3 for these simulations and those of the theoretical ACDC rates (Kürten et al. 2016) are greater than is exhibited in the present and previous work (Benson et al. 2011; Berndt et al., 2010; Kürten et al. 2016; Kirkby et al. 2011), there may be a commonality across this set of experimental work: that contaminants affected the nominally binary measurements. The low dependence of particle formation rate on ammonia (or low 'enhancement factors' e.g. Benson et al., 2011) exhibited in previous work (Benson et al. 2011; Berndt et al. 2010; Kirkby et al. 2011; Kürten et al. 2016) may have been due in part to the influence of contaminants. A 'saturation effect' at high ammonia levels may also act to limit (Kirkby et al. 2011) the ammonia dependence of the nucleation rate. Yet there is congruence of results from a few experiments for high ammonia conditions (see 3.4.1 below.)

The added-dimethylamine data in Fig. 5 show that dimethylamine has a very large effect on N_p, 2 to 3 orders of magnitude (Q_4 = 2.1 sccm for this data). There is a low dependency on dimethylamine abundance where N_p scales approximately linearly with amine mixing ratio. Simulations using DMA_I thermodynamics (Hanson et al. 2017) are also shown in Fig. 5 and simulated N_p mimic fairly well the experimental N_p and its variation with dimethylamine, except perhaps at 30 pptv dimethylamine where simulated N_p is $3x10^7$ cm^{-3}. Coagulation would reduce simulated N_p considerably: with a coagulation rate coefficient of $2x10^{-9}$ cm^3/s, an N_p of $3x10^7$ cm^{-3} results in a coagulation rate of $2x10^{-9}(3x10^7)^2 = 2x10^6$ cm^{-3} s^{-1}. In just five seconds, a third of the simulated particles can coagulate. This rough estimate suggests coagulation is important for those conditions and the effect should be properly evaluated in the simulations.

The dimethylamine results presented in Figs. 4 and 5 are small sets of data and for Fig. 4 dimethylamine was added at a level that challenges the lower range of the dynamic dilution system. Nonetheless, the thermodynamic scheme DMA_I yields cluster concentrations that are consistent with the measured N_p and its trends with dimethylamine level. **Since the** thermodynamics **scheme DMA_I** (Hanson et al. 2017) was **developed by comparing** to the **dimethylamine-H_2SO_4** data of **Glasoe et al. (2015), the present data and the** Glasoe et al. **dimethylamine results are tied together in a semi-quantitative sense.**

3.2.3 Water variation and addition of dimethyl amine.

Shown in Fig. **6 as filled squares are measured N_p vs.** humidity, calculated from the flow rate of the humidified nitrogen. Total flow rate, HONO, and SO_2 levels were kept constant; the humidified flow rate was varied from 0.5 to 2.4

Deleted: experimental results. Failure to mimic

Deleted: poor

Moved (insertion) [15]

Deleted: inaccurate

Deleted: are probably the dominant contributor. We had concluded

Deleted: .,

Deleted: that NH3_II

Deleted: better than NH3_I based on comparisons

Deleted: experimental

Deleted: (

Moved up [4]: 2015).

Deleted: The comparison shown in Fig. 7a indicates that neither satisfactorily represents the full range of the data with NH3_II having particularly overly strong binding free-energies while, relatively speaking, NH3_I is a better approximation of the NH_3-H_2SO_4 cluster binding energies for the present conditions

Deleted: 5

Deleted: .

Moved (insertion) [16]

sLpm. Although the overall data is phenomenologically exponential (the **solid line** in the figure), over limited ranges the data exhibits power dependencies on RH **of between 4 and 6**. A strong dependence of the number of particles on RH is expected for the binary sulfuric acid water nucleating system, and the power dependence here lies at the low end of range (5-to-9) reported by Zollner et al. **(2012). A plot of the size of the leading edge mode vs. humidity is presented in the Supplement (Fig. S1.2.2b).**

A set of data with 2-to-5 pptv dimethylamine added is shown as the diamonds **(filled and open are Q_4=4.2 and 2.1 sccm, respectively)**. There is much less water dependence (approximately linear) when dimethylamine is present which is consistent with theoretical notions (Almeida et al. 2013; Henschel et al. **2016)** that **dimethylamine-H_2SO_4** clusters are not particularly sensitive to H_2O. This postulate has **also** been elucidated in **several other** publications (e.g. Kurten et al. 2008; Coffman and Hegg, 1995). **The data indicates there may be a slightly higher sensitivity to water vapor at the low Q_4 conditions. A complicating factor in fully interpreting this data is that the steady-state H_2SO_4 abundance (the monomer and all its hydrates) changes with RH because its overall diffusivity changes about 10 % as RH varies from 15 to 80 % (Hanson and Eisele, 2000.) More experimental work is needed in this interesting system.**

Supposing there **are** dimethylamine-type base **contaminants** in the putatively base-free experiments (solid squares), it clearly does not reach the single digit pptv level for baseline 52 % RH conditions. Indeed, simulated particle number densities with a level of 0**.005** pptv dimethylamine entering the flow reactor were consistent with the 52% RH, Q_4=4.2 sccm results **(see section 3.3 below).** A set of simulations were run from 0.005 up to 2 pptv dimethylamine and predicted N_p scaled linearly with base level. At the 2 pptv level, an N_p of about 10^7 cm^{-3} was predicted while experimental N_p is $3x10^6$ cm^{-3}. Note that an N_p at the 10^7 cm^{-3} level will be significantly affected by coagulation which is not captured in the simulations.

3.2.4 SO_2.

Particle size and number density were found to depend on SO_2 abundance. Shown in **Fig. 7 is N_p vs.** the flow rate of the SO_2 mixture, Q_1. HONO source flow rate Q_4 was 4.2 sccm for this data. Despite its scatter, the data show the SO_2 level affects both the number of large particles and their size, $D_{V,le}$ **(shown in Fig. S1.2.2c): both increase with [SO_2] and begin to level-off at high [SO_2]. This qualitative behavior is expected as at low SO_2 abundance not all of the OH will react with SO_2 and above a certain level there should not be much more of an effect with increases in SO_2. Young et al. (2008) also report a stronger-than-expected dependence of their results on SO_2 abundance.**

A set of simulations **that includes a reaction between HO_2 and SO_2 is shown as the solid line in Fig. 7. Note that a level of 200 pptv of NH_3 entering the flow reactor was included.** The experimental results show increases with SO_2 that are roughly in line with the model simulations. **Without this reaction the model shows (the dashed line) much smaller increases in N_p (40 % vs. 250 % with the reaction) and in size (Fig. S1.2.2c, 10% vs. 20% with the reaction) as SO_2 increases from 2 to 16 pptv.**

Moved up [16]: humidity, calculated from the flow rate of the humidified nitrogen. Total flow rate, HONO, and SO_2 levels were kept constant; the humidified flow rate was varied from 0.5 to 2.4 sLpm.

Deleted: 8 are the N_p and D_{le} vs.

Deleted: see

Deleted: fit

Deleted: . The power dependence of N_p

Moved (insertion) [17]

Moved up [17]: A strong dependence of the number of particles on RH is expected for the binary sulfuric acid water nucleating system, and the power dependence here lies at the low end of range (5-to-9) reported by Zollner et al.

Deleted: is between 4 and 6 while $D_{V,le}$ varies from 5 nm to about 10 nm; there appears to be a rise in both above 80 % RH.

Moved (insertion) [18]

Deleted: .

Moved up [18]: There is much less water dependence (approximately linear) when dimethylamine is present which is consistent with theoretical notions (Almeida et al. 2013; Henschel et al.

Deleted: 2016). This indicates

Deleted: that lead to large particles

Deleted: when dimethyl amine is present, because the amine is a much better base than H_2O and nucleation associated with a strong acid-base interaction is preferred.

Deleted: previous

Deleted:

Deleted: is

Deleted: contaminant

Deleted: , as shown in the Supplement

Deleted: 003

Deleted: .

Deleted: well

Formatted: Font: Not Bold

Moved (insertion) [7]

Moved (insertion) [8]

Deleted: 3.2.6 Variations of dimethylam ... [27]

Moved (insertion) [9]

Moved (insertion) [10]

The simulation assumed a value of $3x10^{-17}$ cm^3/s for $k_{HO2+SO2}$. **There is disagreement** whether HO_2 reacts with SO_2 as well as potential end products (Chen et al. 2014; Kurten et al. 2011); we assumed H_2SO_4 and OH. **Experimental** values for this rate coefficient range from upper limits of $1x10^{-18}$ cm^3/s (Graham et al. 1979) and $2x10^{-17}$ cm^3/s (Burrows et al. 1979), to a value of $8x10^{-16}$ cm^3/s (Payne et al. 1973). A heterogeneous reaction occurring in the particles involving SO_2 would help explain the dependence of $D_{V,le}$ on SO_2 abundance **(Fig. S1.2.2c) while leaving N_p undisturbed.**

Moved (insertion) [11]

Moved (insertion) [12]

Deleted: with

3.3 Characteristics of a potential contaminant

Shown in Fig. 8 are the experimental N_p as a function of HONO from Fig. 4a along with model simulated N_p. The simulations were run for NH_3 at 0 and 200 pptv using NH3_52 thermodynamics and for dimethylamine at 0.005 pptv using DMA_I thermodynamics (Hanson et al. 2017)**. The experimental data is for nominally-clean conditions.**

Formatted: English (U.K.)

Deleted:) at Q_4 = 2 sccm with dimethylamine at levels of 5 and 10 pptv predict N_p of $5x10^6$ cm^{-3} and $1x10^7$ cm^{-3}, respectively. These compare favorably with the measured N_p at 5 and 10 pptv of 2.5 and 5 $x10^6$ cm^{-3}, respectively.

Formatted: English (U.K.)

Deleted: modeled

Formatted: English (U.K.)

Formatted: English (U.K.)

Deleted: reduced with a proper treatment of particle-particle collisions.

Moved up [15]: Nonetheless, the thermodynamic scheme DMA_I yields cluster concentrations that are consistent with the measured N_p and its trends with dimethylamine level.

Deleted: Scheme DMA_I was able to mimic the dimethylamine-H_2SO_4 data

Deleted: ., tying that data

Moved up [13]: ¶
Since effects due to adding dimethylamine at the single-digit pptv level are large, it would be desirable to experimentally investigate amine additions at lower levels.

Deleted:

Deleted: present data.

Deleted: With the current dynamic dilution system base additions at levels lower than a few pptv are swamped by the precision uncertainty in flowmeter readings.

Moved up [14]: More results from these types of experiments await further improvement in the dimethylamine delivery system.

Deleted: ¶

Deleted: 3

Deleted: 11

The **simulations with NH_3 at 200 pptv yield N_p similar to the experimental and furthermore dependencies upon HONO align with experimental dependencies. The powerful nucleator dimethylamine entering the flow reactor at 5 ppqv (1.2 $x10^5$ cm^{-3}) also yields a simulated N_p at Q_4 = 4.2 sccm close to the experimental N_p of about $2.5x10^4$ cm^{-3}. The variation of predicted N_p with HONO, however, is disparate from the experimental variation, where the simulated N_p levels off at high values of Q_4. This leveling off is due, at least in part, to a simple number limitation: the largest simulated N_p is $4x10^4$ cm^{-3} which is about one third of the number density of dimethylamine molecules introduced. A strict limit would be reached depending on how many dimethylamine molecules are in each particle. Nonetheless, the simulations suggest the contaminant acts more like ammonia than dimethylamine.**

While the presence of 200 pptv ammonia is consistent with the experimental N_p, methylamine has comparable power dependencies on acid. These are plotted as the purple circles in Fig. 8 where the methylamine nucleation rates were taken from the expression in Table S2 of Glasoe et al**. (2015) and a 4 s nucleation time was applied. Since it is significantly less powerful than dimethylamine, a larger abundance of 0.5 pptv is needed to give N_p comparable** to the **experiment and the full range of Q_4 is covered, assuming scavenging of methylamine by clusters would be minimal. An impurity with an abundance of a fraction of a pptv may last a long time due to a low evaporation rate. These considerations would make methylamine (or perhaps another primary amine) a suitable candidate for a potential gas-phase base contaminant in PhoFR. Of course, whether the contaminant is ammonia or methylamine (or perhaps a combination) cannot be determined at this time. However, it appears that studying the primary amines would be interesting in this context as well as for understanding their effects on sulfuric acid nucleation rates. The Supplement (S9) presents some more discussion on the effects of SO_2.**

3.4 Comparison to previous results.

A number of previous results are compiled along with the present measurements in Fig. **9** for nominally base-free conditions. The present results are assigned the simulated H_2SO_4 value in the center of the reactor and at 30 cm into the illuminated region. The nucleation rate J was taken to be N_p divided by the time the center of the flow travels from 20 to 40

cm, 4 s. This time is presumed to apply for the nominally clean conditions here. On the other hand, with base added intentionally, significant nucleation may also occur in the 0 to 20 cm region where base abundance is high. Uncertainties in J are probably on the order of a factor of 2. Uncertainty in H_2SO_4 is about a factor of two, based on the calculated values at 15 and 60 cm, which are -49 and +106 %, resp., from the 30 cm value. The radial profile of H_2SO_4 at 30 cm axial distance is flat from the center out to a radius of 1.7 cm. **See the Supplement for radial profiles of H_2SO_4 (Fig. S1.3.3).**

The experimental data in Fig. **9** were taken over a range of temperatures, 288 to 300 K, and relative humidities, 2.3 to 75 % RH; conditions indicated in the legend. The present results extrapolate to rates that are in fair agreement with Benson et al. 2009 and much of the CLOUD data set (Kirkby et al. 2011; **Kürten** et al. 2016) except for the 40 % RH at 298 K data. The bulk-source H_2SO_4 data reported by Zollner et al. is included for reference; it was corrected from 38% RH to 52 % RH, increasing by about a factor of 5 using a RH^5 dependency. The difference between the bulk-source and present photolytic H_2SO_4 is about 4 orders of magnitude; the **Kürten** et al. (2016) 40 % RH data is closest to this set of bulk data, within about two orders of magnitude.

There is apparent agreement of several data sets for H_2SO_4 concentrations of 10^8 to 10^9 cm^{-3}: our lowest J (and the extrapolation of our data, dotted line), Yu et al. (2017), Benson et al. (2009), **Kürten** et al. (2016) and Kirkby et al. (2012) but it is complicated by the wide range of relative humidities: 2.3 % RH up to 75 % RH. **The data of Young et al. (2008) suggests a very low contamination level however there are unresolved issues in measured [H_2SO_4] (see the factor of ten disparity in their Fig. 5).** Lack of experimental water dependencies and assessment of base-levels makes drawing conclusions **from these comparisons** fraught with difficulty. Nonetheless, it is interesting that the dependencies of J on sulfuric acid level are similar in many of these studies. This suggests there is an underlying similarity in particle formation conditions such as contaminant identity and level (which seems unlikely) or the critical cluster's H_2SO_4-content is not particularly sensitive to the type or abundance of the contaminant.

Deleted: previous

Deleted: 11

Deleted: Kurten

Deleted: Kurten

Deleted:

Deleted: Kurten

3.4.1 Comparison of nucleation rates for added ammonia

Plotted in Fig. 10 are nucleation rates vs. ammonia abundance for measurements at low [H_2SO_4], $5x10^7$ and $1.5x10^8$ cm^{-3}, and temperatures between 288 and 293 K. Also plotted are predictions according to the present data using the box-model and methodology presented in Hanson et al. (2017). The experimental data from the CLOUD project for 292.5 K were taken from Dunne et al. (2017) and were also presented by Kürten et al. (2016). The Benson et al. (2009, 2011) work was performed at 288 K and significant extrapolation of nucleation rates were applied to get comparable sulfuric acid concentrations (see the caption). The Berndt et al. (2011) work was performed at 293 K and extrapolation was needed to get comparison rates for the $1.5x10^8$ cm^{-3} [H_2SO_4] conditions.

The model predictions using the NH3_52 thermodynamics developed here gives rates that are congruent with the CLOUD data and with Berndt et al. (2011) while NH3_I thermodynamics (calculated only for [H_2SO_4] = $1.5x10^8$ cm^{-3}) gives rates too high by two-to-three orders of magnitude. NH3_I is a set of ammonia-sulfuric acid thermodynamics derived in Hanson et al. (2017) that skirted the lower limit of the Glasoe et al. (2015) ammonia data set. Benson et al.

(2009, 2011) is quite disparate and a temperate correction would lessen the discrepancy for the set of data at the low H_2SO_4 but it would worsen it at the higher H_2SO_4.

With the box-model predictions using NH3_52 thermodynamics serving as a bridge, the present ammonia-added data agrees with both the CLOUD data (Kürten et al., 2016; Dunne et al. 2017) and the Berndt et al. (2011) data. Since the box-model rates using NH3_I thermodynamics (Hanson et al. 2017) are much too high, we can conclude that the Glasoe et al. (2015) ammonia data set it was based on does not agree with the present measurements. Recently, Kürten (2019) concluded that the NH3_II (stronger binding than NH3_I) thermodynamics of Hanson et al. (2017) yields nucleation rates much higher than the CLOUD measurements.

4 Summary

We presented a new experimental apparatus for studying particle formation involving photolytically-formed H_2SO_4 vapor and results show the system is reproducible and responds to changes in water, HONO and SO_2 concentrations largely as expected. Modeled particle formation rates could be made congruous with experimental observations by including either dimethylamine at a level of **5x10^{-15}** mole fraction or NH_3 at a level of **~2x10^{-10}** mole fraction. Also, the dependence of N_p on SO_2 level was best explained by a reaction between HO_2 and SO_2 that yields (ultimately) H_2SO_4 and OH with a rate coefficient of 3x10^{-17} cm^3/s.

Comparison of the present results to other photolytic H_2SO_4 experiments yields several suppositions. Their divergence from the bulk-source data of Zollner et al. **(2012)** suggests these experiments are not clean enough and/or they are subject to an unknown reaction or photochemistry. The similarity of the present results to those of Benson et al. (2009), Kirkby et al. (2011), **Kürten** et al. (2016) and Yu et al. (2017) suggests a common element that affects nucleation beyond what bulk-source H_2SO_4 experiments reveal. The outlier results of Berndt et al. (2010, 2014) and Benson et al. (2011) may suffer from relatively high level of contaminants: Berndt et al. (2014) suggested that a pptv-level of amine could have been present in their experiment. As can be seen in Fig. **9**, there is a remarkable agreement of the H_2SO_4 power dependencies for Kirkby et al. (2011), Yu et al. (2017), and the present results. This may be due to a similarly-sized critical cluster across these studies.

Side products from photolytic generation of H_2SO_4 that enhance nucleation were suggested by Berndt et al. (2008), however, **Sipilä** et al. (2010) found no difference between nucleation rates whether H_2SO_4 was produced photolytically or taken from a bulk source. **Yet much of** the **Sipilä** et al. (2010) **photolytic** nucleation rates **are** many orders of magnitude too high for the putative binary system (**see Fig. 9 comparing** the present results, the Zollner et al. (2012) bulk-liquid data, **Yu et al. (2017) and** results from the CLOUD experiment**;** Kirkby et al**.(2011), Kürten** et al**.(2016).) With** the **exception of their bulk 298 K 30% RH results, the Sipilä** et al. (2010) data largely **overlap** the Benson et al. (2011) and Berndt et al. (2014) data**, and** probably also **suffer** from amine contaminants at the pptv-level.

The total particle number strongly depended on relative humidity with RH^4 and RH^6 power relationships over RH ranges of 15 to 35 % and 40 to 77%, respectively. The CLOUD 298 K **results (Kürten** et al**., 2016) show** a power dependency of 4

Deleted: 3x10
Deleted: 10
Deleted: Kurten
Deleted: 11
Deleted: Sipila
Deleted: Since then,
Deleted: Sipila
Deleted: have been seen to be
Deleted: i.e., extrapolation of
Deleted: (
Deleted: ., Kurten
Deleted: 2017) and Yu et al. (2017).) Since
Deleted: Sipila
Deleted: overlaps
Deleted: , it
Deleted: suffers
Deleted: data reported by Kurten
Deleted: . (2017) shows

on RH from 40 to 75 % at 298 K in rough agreement with the present results. Yu et al. **(2017)** reported a nucleation rate that depended linearly on RH that seems to be out of line with these other data sets.

The weak dependence of N_p on added NH_3 **near room temperature,** also reflected in **a few** other studies (Kirkby et al. **2011; Kürten** et al. **2016,** Benson et al., **2011), is probably due** to **a contaminant** that **overwhelms** ammonia-**induced nucleation, especially at low levels of added ammonia. We surmised that a contaminant in our system is not consistent with dimethylamine but** is consistent with **a few hundred pptv of ammonia; alternatively, we postulated that 0.5 pptv of methylamine could also be responsible.**

The model simulations with NH_3-H_2SO_4 thermodynamic schemes NH3_I and**, because it is stronger,** NH3_II (Hanson et al. 2017)**, result** in N_p that **greatly exceed the present experimental results.** With the simulations serving as a bridge between these two experiments, we conclude that the present experimental data and the Glasoe et al. **(2015)** NH_3-H_2SO_4 results do not agree. Glasoe et al. **(2015) noted that** their NH_3-H_2SO_4 **nucleation rates were much higher than** those of Ball et al. **(1999)** and Zollner et al. **(2012), but with** the present results **as a backdrop the Glasoe et al. criticisms of those two studies are blunted.** In hindsight we postulate **an** avenue for an amine contamination in the Glasoe et al. **(2015)** ammonia experiments: several amino-compounds were studied in succession **using** the same dynamic dilution system. **Since** ammonia **was used** between **amines, holdover of the** amine **is possible and even small levels would significantly boost particle numbers, compromising** the ammonia-sulfuric acid system **measurements.** Note that in the present experimental setup, there were **two** dynamic dilution systems**, one dedicated** for ammonia and **one** for dimethylamine.

Additions of dimethylamine resulted in large abundances of particles which limited the range of conditions we were able to study. The number densities are such that a model with proper treatments of coagulation and cluster- cluster collisions is needed to fully interpret the results. Nonetheless, the experimental results are in decent agreement with model simulations using the thermodynamic scheme (DMA_I, Hanson et al., 2017) that best captured the Glasoe et al. (2015) dimethylamine-H_2SO_4 experimental results. We found low RH dependencies when dimethylamine was added**,** in line with expectations. **Note** the **details** of **this** preliminary finding **need further work: (i) RH affects the steady-state sulfuric acid** and **(ii)** coagulation effects need to be **properly evaluated**.

Atmospheric implications of the present work are of a qualitative nature. The current work suggests that nucleation rates in the NH_3-H_2SO_4 system **for a few studies can be seen to converge but more measurements near room temperature** are **needed to aid the development of ammonia-sulfuric acid thermodynamics (e.g. this work, Hanson et al. 2017; Kürten, 2019). We concluded that the** experimental nucleation **rates in this system from** Glasoe et al. (2015) **are discordant.** On the other hand, as alluded to in the previous paragraph, the current work is consistent with the Glasoe et al. **(2015)** dimethylamine-H_2SO_4 results. Also, the much-predicted low RH dependency for dimethylamine-H_2SO_4 nucleation finds experimental corroboration here. Finally, even if the reaction of HO_2 with SO_2 occurs with a rate coefficient of $1x10^{-16}$ cm^3 s^{-1}, it is probably an insignificant source of atmospheric hydroxyl radicals and oxidized sulfur compounds.

In the future, a series of measurements **in the dimethylamine-H_2SO_4 system** with added dimethylamine at fractional pptv levels **and low relative humidities** are planned. We also plan to study the relative humidity dependence of ammonia-

Deleted: A nearly linear

Deleted: was found which is

Deleted: several

Deleted: ., Kurten

Deleted: .,

Deleted: .). This departs from the bulk-liquid experiments of Glasoe et al. who report a 1.6 NH_3-power dependency and the ACDC model predicts a power dependency of 2

Deleted: 3 (Kurten et al., 2017), albeit at lower H_2SO_4. At constant NH_3, we found power ... [28]

Deleted: found by Glasoe et al. (2015) and ... [29]

Deleted:

Deleted: nucleation initiated by sulfamic a ... [30]

Deleted:) resulted

Deleted: exceeded experiment for a large ... [31]

Deleted: discussed the discrepancies between

Deleted: results and

Deleted: ., but now, since the Glasoe et al ... [32]

Deleted: , we conclude that the Glasoe et a ... [33]

Deleted: can

Deleted: a possible

Deleted: with

Deleted: and

Deleted: experiments were performed in

Deleted: experiments. Measurements in

Deleted: would be most vulnerable to the ... [34]

Deleted: separate

Deleted: dimethylamine

Deleted: but it should be emphasized that

Deleted: linearity

Deleted: the RH dependence of N_p is a

Deleted: on these N_p values

Deleted: investigated with a proper coagu ... [35]

Deleted: still uncertain and need further

Deleted: investigation. Furthermore, we c ... [36]

Deleted: rate expression eq. 3 of

Deleted: likely overestimates nucleation i ... [37]

Deleted: of particles

Deleted: to better determine H_2SO_4 and a ... [38]

induced H_2SO_4 nucleation as well as variations of temperature on both amine- and ammonia-addition nucleation. In the long term, the system developed here will be used in particle growth studies where nm-diameter particles prepared in the Glasoe et al. **(2015)** apparatus are directed through PhoFR along with target organic compounds.

Data availability. All data presented in this manuscript are available by contacting the **corresponding author**.

Deleted: authors

Author contribution.

HA and JV built the particle detector and performed preliminary experiments, MA helped design and carry out experiments, SM carried out added-NH_3 experiments and helped with the manuscript, JK helped develop the photochemical module, and DH developed and ran the simulations, developed and carried out experiments and prepared the manuscript with contributions from all co-authors. The authors declare that they have no conflict of interest.

Acknowledgements.

Thanks to C. Grieves, C. Ward, N. Hoffmann and S. Thao for performing verification experiments that lead to improvements in the deployment of the DEG system and T. Otsego for data analysis. Thanks to T. Kukowski for programming help on the numerical model. Thanks to Y. Melka and N. Clark for their work on the Python program that accumulates and displays particle counter data. We are grateful to Dr. M. Stolzenburg and Prof. P. McMurry for comments on the manuscript and for lending their expertise and guidance during the course of this work.

Deleted: ¶
¶

References

Almeida, J., Schobesberger, S., Kürten, A., Ortega, I. K., Kupiainen-Määttä, O., Praplan, A. P., Adamov, A., Amorim, A., Bianchi, F., Breitenlechner, M., David, A., Dommen, J., Donahue, N. M., Downard, A., Dunne, E. M., Duplissy, J., Ehrhart, S., Flagan, R. C., Franchin, A., Guida, R., Hakala, J., Hansel, A., Heinritzi, M., Henschel, H., Jokinen, T., Junninen, H., Kajos, M., Kangasluoma, J., Keskinen, H., Kupc, A., Kurtén, T., Kvashin, A. N., Laaksonen, A., Lehtipalo, K., Leiminger, M., Leppä, J., Loukonen, V., Makhmutov, V., Mathot, S., McGrath, M. J., Nieminen, T., Olenius, T., Onnela, A., Petäjä, T., Riccobono, F., Riipinen, I., Rissanen, M., Rondo, L., Ruuskanen, T., Santos, F. D., Sarnela, N., Schallhart, S., Schnitzhofer, R., Seinfeld, J. H., Simon, M., Sipilä, M., Stozhkov, Y., Stratmann, F., Tomé, A., Tröstl, J., Tsagkogeorgas, G., Vaattovaara, P., Viisanen, Y., Virtanen, A., Vrtala, A., Wagner, P. E., Weingartner, E., Wex, H., Williamson, C., Wimmer, D., Ye, P., Yli-Juuti, T., Carslaw, K. S., Kulmala, M., Curtius, J., Baltensperger, U., Worsnop, D. R., Vehkamäki, H., and Kirkby, J.: Molecular understanding of sulphuric acid-amine particle nucleation in the atmosphere, Nature, 502, 359–363, https://doi.org/10.1038/nature12663, 2013.

Moved (insertion) [19]

Moved (insertion) [20]

Deleted: Almeida, J., S. Schobesberger, A. Kurten, I. K. Ortega, O. Kupiainen-Maatta, A. P.

Ball, S. M., D. R. Hanson, F. L. Eisele, and Peter H. McMurry. "Laboratory Studies of Particle Nucleation - Initial Results for H_2SO_4, H_2O, and NH_3 Vapors." *J Geophys Res* 104 (D19): 23, 718, 1999.

Benson, D. R., **Erupe, M.E., and S.-H Lee. "Laboratory-measured H_2SO_4, NH_3, H_2O ternary homogeneous nucleation rates: Initial observations" *Geophys. Res. Lett.* 36, L15818, doi:10.1029/2009GL038728, 2009.**

Benson, D. R., J. H. Yu, A. Markovich, and S. -H Lee. "Ternary Homogeneous Nucleation of H_2SO_4, NH_3, and H_2O Under Conditions Relevant to the Lower Troposphere." *Atmos Chem Phys* 11 (10): 4755-4766. doi:10.5194/acp-11-4755-2011, 2011.

Berndt, T., F. Stratmann, **Brasel, S.,** J. **Heintzenberg, A. Laaksonen, M. Kulmala "SO_2: oxidation products other than H2SO4 as a trigger for new particle formation. Part 1: Laboratory investigations." *Atmos Chem Phys* 8: 6365-6374. doi:10.5194/acp-8-6365-2008, 2008.**

Berndt, T., F. Stratmann, M. Sipilä, J. Vanhanen, T. Petaejae, J. Mikkilae, A. Gruener, **Spindler, G., Mauldin III, R., Curtius, J., Kulmala, M., and Heintzenberg, J.:** "Laboratory Study on New Particle Formation from the Reaction OH + SO_2: Influence of Experimental Conditions, H_2O Vapour, NH_3 and the Amine Tert-Butylamine on the overall Process." *Atmos Chem Phys* 10 (15): 7101-7116. doi:10.5194/acp-10-7101-2010, 2010.

Berndt, T., Sipilä, M., Stratmann, F., Petäjä, T., Vanhanen, J., Mikkilä, J., Patokoski, J., Taipale, R., Mauldin III, R.L., and M. Kulmala, Enhancement of atmospheric H2SO4/H2O nucleation: organic oxidation products versus amines. Atmos Chem Phys, 14, 751-764. doi:10.5194/acp-14-751-2014, 2014.

Burrows, J. P., D. I. Cliff, G. W. Harris, B. A. Thrush, and J. P. T. Wilkinson. "Atmospheric Reactions of the HO_2 Radical Studied **By** Laser MRS." *Proc Royal Soc of London. Ser A*, 368: 463-481, 1979.

Chen, X., Cen Tao, Li Zhong, Ya Gao, Wei Yao and Shujin Li, Theoretical study on the atmospheric reaction of SO2 with the HO2 and HO2·H2O complex formation HSO4 and H2SO3, Chem. Phys. Lett., 608, 2720276 2014.

Coffman, D. J. and D. A. Hegg. "A Preliminary Study of the Effect of Ammonia on Particle Nucleation in the Marine Boundary Layer." *J. Geophys. Res., [Atmospheres]* 100 (D4): 7147-7160. doi:10.1029/94JD03253, 1995.

Dunne, E. M., Gordon, H., Kürten, A., Almeida, J., Duplissy, J., Williamson, C., Ortega, I. K., Pringle, K. J., Adamov, A., Baltensperger, U., Barmet, P., Benduhn, F., Bianchi, F., Breitenlechner, M., Clarke, A., Curtius, J., Dommen, J., Donahue, N. M., Ehrhart, S., Flagan, R. C., Franchin, A., Guida, R., Hakala, J., Hansel, A., Heinritzi, M., Jokinen, T., Kangasluoma, J., Kirkby, J., Kulmala, M., Kupc, A., Lawler, M. J., Lehtipalo, K., Makhmutov, V., Mann, G., Mathot, S., Merikanto, J., Miettinen, P., Nenes, A., Onnela, A., Rap, A., Reddington, C. L. S., Riccobono, F., Richards, N. A. D., Rissanen, M. P., Rondo, L., Sarnela, N., Schobesberger, S., Sengupta, K., Simon, M., Sipilä, M., Smith, J. N., Stozkhov, Y., Tomé, A., Tröstl, J., Wagner, P. E., Wimmer, D., Winkler, P. M., Worsnop, D. R., and Carslaw, K. S.: Global atmospheric particle formation from CERN CLOUD measurements, Science, 354, 1119-1123, 2016.

Eisele F. L. and D. J. Tanner, Measurement of the Gas Phase Concentration of H_2SO_4 and Methane Sulfonic Acid and estimates of H_2SO_4 Production and Loss in the Atmosphere, J. Geophys. Res. D, 98, 9001-9010, 1993.

Moved up [19]: Praplan, A.

Formatted: Indent: Left: -0.1", Hanging: 0.2"

Deleted: Adamov, et al. "Molecular Understanding of Sulphuric Acid-Amine Particle Nucleation in the Atmosphere," *Nature (London, United Kingdom)* 502 (7471): 359-363. doi:10.1038/nature12663. 2013.¶

Formatted: Subscript

Formatted: Subscript

Formatted: Subscript

Formatted: Subscript

Moved (insertion) [21]

Formatted: Font: Italic

Formatted: Indent: Left: -0.1", Hanging: 0.2"

Formatted: Subscript

Formatted: Subscript

Formatted: Subscript

Formatted: Subscript

Deleted: M. Sipilae,

Formatted: Indent: Left: -0.1", Hanging: 0.2"

Deleted: et al.

Formatted: Subscript

Formatted: Subscript

Formatted: Subscript

Deleted: .,

Formatted: Indent: Left: -0.1", Hanging: 0.2"

Deleted: HO_2

Deleted: Buy

Formatted: Indent: Left: -0.1", Hanging: 0.2"

Moved (insertion) [22]

Formatted: Font: Not Italic

Deleted: Ehrhart, S. et al.: Comparison of the SAWNUC model with CLOUD measurements of sulphuric acid-water nucleation, J. Geophys.

Ehrhart, S., Ickes, L., Almeida, J., Amorim, A., Barmet, P., Bianchi, F., Dommen, J., Dunne, E. M., Duplissy, J., Franchin, A., Kangasluoma, J., Kirkby, J., Kürten, A., Kupc, A., Lehtipalo, K., Nieminen, T., Riccobono, F., Rondo, L., Schobesberger, S., Steiner, G., Tomé, A., Wimmer, D., Baltensperger, U., Wagner, P. E., and Curtius, J.: Comparison of the SAWNUC model with CLOUD measurements of sulphuric acid water nucleation, J. Geophys. Res.-Atmos., 121, 12401–12414, https://doi.org/10.1002/2015JD023723, 2016.

Febo, A., Perrino, C., Sparapani, R. and Gherardi, M.: Evaluation of a High-Purity and High-Stability Continuous Generation System for Nitrous Acid, Environ. Sci. Tech., 29, 2390-2395, 1995.

Friese, E. and Ebel, A., Temperature Dependent Thermodynamic Model of the System $H^+-NH_4^+-Na^+-SO_4^{2-}-NO_3^--Cl^--H_2O$, J. Phys. Chem. A, 114, 11595-11631, 10.1021/jp101041j, 2010.

Freshour, N., K. K. Carlson, Y. A. Melka, S. Hinz, B. Panta, and D. R. Hanson "Quantifying Amine Permeation Sources with Acid Neutralization: Calibrations and Amines Measured in Coastal and Continental Atmospheres." *Atmos. Meas. Tech.* 7: 3835-3861, 2014.

Glasoe, W. A., K. Volz, B. Panta, N. Freshour, R. Bachman, D. R. Hanson, P. H. McMurry, and C. N. Jen. "Sulfuric Acid Nucleation: An Experimental Study of the Effect of Seven Bases." *J. Geophys. Res. D.* 120, 2015.

Graham, R.A., A M Winer, R Atkinson, and J Pitts Jr. "Rate Constants for the Reaction of HO_2 with HO_2, SO_2, CO, N_20, Trans-2-Butene, and 2,3-Dimethyl-2-Butene at 300 K." *J. Phys. Chem.* 83, 1979.

Hanson, D. R., I. Bier, B. Panta, C. N. Jen, and P. H. McMurry. "Computational Fluid Dynamics Studies of a Flow Reactor: Free Energies of Clusters of Sulfuric Acid with NH_3 and Dimethylamine." *J. Phys. Chem. A* 121 (20): 3976, 2017.

Henschel, H., T. Kurten, and H. Vehkamaki "Computational Study on the Effect of Hydration on New Particle Formation in the Sulfuric Acid/Ammonia and Sulfuric Acid/Dimethylamine Systems," *J. Phys. Chem. A* 120, 1886-1896. doi:10.1021/acs.jpca.5b11366, 2016.

Intergovernmental Panel on Climate Change (2013), Climate Change 2013: IPCC 5th Assessment Report (AR5), Edited, 2013.

Jiang, J., M. Chen, C. Kuang, M. Attoui, and P. H. McMurry. "Electrical Mobility Spectrometer using a Diethylene Glycol Condensation Particle Counter for Measurement of Aerosol Size Distributions Down to 1 Nm." *Aerosol Science and Technology* 45 (4): 510-521. doi:10.1080/02786826.2010.547538, 2011.

Kirkby, J., **Curtius, J., Almeida, J., Dunne, E., Duplissy, J., Ehrhart, S., Franchin, A., Gagné, S., Ickes, L., Kürten, A., Kupc, A., Metzger, A., Riccobono, F., Rondo, L., Schobesberger, S., Tsagkogeorgas, G., Wimmer, D., Amorim, A., Bianchi, F., Breitenlechner, M., David, A., Dommen, J., Downard, A., Ehn, M., Flagan, R.C., Haider, S., Hansel, A., Hauser, D., Jud, W., Junninen, H., Kreissl, F., Kvashin, A., Laaksonen, A., Lehtipalo, K., Lima, J., Lovejoy, E. R., Makhmutov, V., Mathot, S., Mikkilä, J., Minginette, P., Mogo, S., Nieminen, T., Onnela, A., Pereira, P., Petäjä, T., Schnitzhofer, R., Seinfeld, J. H., Sipilä, M., Stozhkov, Y., Stratmann, F., Tomé, A., Vanhanen, J., Viisanen, Y., Vrtala, A., Wagner, P. E., Walther, H., Weingartner, E., Wex, H., Winkler, P. M., Carslaw, K. S., Worsnop, D. R.,**

Moved up [21]: *Res.*

Formatted: Font: Italic

Deleted: Atmos., 121, 2016.¶

Formatted: Indent: Left: -0.1", Hanging: 0.2"

Deleted: .:

Formatted: Superscript

Formatted: Subscript

Formatted: Superscript

Formatted: Superscript

Formatted: Subscript

Formatted: Superscript

Formatted: Subscript

Formatted: Superscript

Formatted: Superscript

Formatted: Subscript

Moved (insertion) [23]

Formatted: Subscript

Deleted: et al. "Role of Sulphuric Acid, Ammonia and Galactic Cosmic Rays in Atmospheric Aerosol Nucleation." *Nature* 476: 429-433. doi:10.1038/nature10343, 2011.

Baltensperger, U., and Kulmala, M.: Role of sulphuric acid, ammonia and galactic cosmic rays in atmospheric aerosol nucleation, Nature, 476, 429–435, https://doi.org/10.1038/nature10343, 2011..

Kreyling, W. G., Semmler-Behnke, M. and Moller, W.: Ultrafine Particle-Lung Interactions: Does Size Matter? J. Aerosol Medicine, 19, 74-83, 10.1089/jam.2006.19.74, 2006.

Kuang, C., M. Chen, J. Zhao, J. Smith, P. H. McMurry, and J. Wang. "Size and Time-Resolved Growth Rate Measurements of 1 to 5 Nm Freshly Formed Atmospheric Nuclei." *Atmospheric Chemistry and Physics* 12 (7): 3573-3589. doi:10.5194/acp-12-3573-2012, 2012.

Kulmala, M., H. Vehkamaki, T. Petaja, M. Dal Maso, A. Lauri, V. -M Kerminen, W. Birmili, and P. H. McMurry. "Formation and Growth Rates of Ultrafine Atmospheric Particles: A Review of Observations." *Journal of Aerosol Science* 35 (2): 143-176. doi:10.1016/j.jaerosci.2003.10.003, 2004.

Kürten, A., **L. Rondo, S. Ehrhart, and J. Curtius, "Calibration of a Chemical Ionization Mass Spectrometer for the Measurement of Gaseous Sulfuric Acid" J. Phys. Chem. A, 2012, 116, 6375−6386, dx.doi.org/10.1021/jp212123n.**

Kürten, A., C. Williamson, J. Almeida, J. Kirkby, and J. Curtius. "On the Derivation of Particle Nucleation Rates from Experimental Formation Rates." *Atmospheric Chemistry and Physics* 15 (8): 4063-4075. doi:10.5194/acp-15-4063-2015, 2015.

Kürten, A., **Bianchi, F., Almeida, J., Kupiainen-Määttä, O., Dunne, E. M., Duplissy, J., Williamson, C., Barmet, P., Breitenlechner, M., Dommen, J., Donahue, N. M., Flagan, R. C., Franchin, A., Gordon, H., Hakala, J., Hansel, A., Heinritzi, M., Ickes, L., Jokinen, T., Kangasluoma, J., Kim, J., Kirkby, J., Kupc, A., Lehtipalo, K., Leiminger, M., Makhmutov, V., Onnela, A., Ortega, I. K., Petäjä, T., Praplan, A. P., Riccobono, F., Rissanen, M. P., Rondo, L., Schnitzhofer, R., Schobesberger, S., Smith, J. N., Steiner, G., Stozhkov, Y., Tomé, A., Tröstl, J., Tsagkogeorgas, G., Wagner, P. E., Wimmer, D., Ye, P., Baltensperger, U., Carslaw, K., Kulmala, M., and Curtius, J.: Experimental particle formation rates spanning tropospheric sulfuric acid and ammonia abundances, ion production rates and temperatures, J. Geophys. Res.-Atmos., 121, 12377–12400, https://doi.org/10.1002/2015JD023908, 2016.**

Kürten, A., **Li, C., Bianchi, F.,** Curtius, **J., Dias, A., Donahue, N. M., Duplissy, J., Flagan, R. C., Hakala, J., Jokinen, T., Kirkby, J., Kulmala, M., Laaksonen, A., Lehtipalo, K., Makhmutov, V., Onnela, A., Rissanen, M. P., Simon, M., Sipilä, M., Stozhkov, Y., Tröstl, J., Ye, P., and** McMurry, **P. H.:** New **particle formation** in the **sulfuric acid-**dimethylamine-water **system: reevaluation** of CLOUD **chamber measurements** and **comparison** to an **aerosol nucleation** and **growth model,** Atmos. Chem. Phys., **18, 845–863, https://**doi.**org/**10.5194/acp-18-845-2018, 2018.

Kürten, A. New particle formation from sulfuric acid and ammonia: nucleation and growth model based on thermodynamics derived from CLOUD measurements for a wide range of conditions, Atmos. Chem. Phys., 19, 5033–5050, 2019. https://doi.org/10.5194/acp-19-5033-2019

Kurten, T., V. Loukonen, H. Vehkamaki, and M. Kulmala. "Amines are Likely to Enhance Neutral and Ion-Induced Sulfuric Acid-Water Nucleation in the Atmosphere More Effectively than Ammonia." *Atmospheric Chemistry and Physics* 8 (14): 4095-4103. doi:10.5194/acp-8-4095-2008, **2008**.

Formatted: Indent: Left: -0.1", Hanging: 0.2"

Deleted: . et al. "Experimental Particle Formation Rates Spanning Tropospheric Sulfuric Acid and Ammonia Abundances, Ion Production Rates, and Temperatures," *J.*

Moved up [22]: Geophys. Res.

Formatted: Font: Not Italic

Deleted: 121 (20): 12,400. doi:10.1002/2015JD023908, 2016.

Deleted: et al., J.

Deleted: . H.

Deleted: "

Deleted: Particle Formation

Deleted: Sulfuric Acid–

Deleted: –

Deleted: System: Reevaluation

Deleted: Chamber Measurements

Deleted: Comparison

Deleted: Aerosol Nucleation

Deleted: Growth Model"

Formatted: Font: Not Italic

Deleted: .

Deleted: :

Deleted:

Formatted: Indent: Left: -0.1", Hanging: 0.2"

Deleted: 2018

Kurten, T., J. R. Lane, S. Jørgensen, and H. G. Kjaergaard, A Computational Study of the Oxidation of SO2 to SO3 by Gas-Phase Organic Oxidants, J. Phys. Chem. A, 115, 8669–8681, 2011. dx.doi.org/10.1021/jp203907d

Larriba, A., Hogan, C. and de **Lamora**, J.: The Mobility–Volume Relationship below 3.0 nm Examined by Tandem Mobility–Mass Measurement, Aerosol Science and Technology, 45, 453-467, 2010.

Lovejoy, E. R., Hanson, D. R. and Huey, L. G.: Kinetics and Products of the Gas-Phase Reaction of SO_3 with Water, J. Phys. Chem., 100, 19911-19916, 1996.

McMurry, P. H. "New Particle Formation in the Presence of an Aerosol: Rates, Time Scales, and Sub-0.01 Um Size Distributions," *Journal of Colloid and Interface Science* 95 (1): 72-80. doi:10.1016/0021-9797(83)90073-5, 1983.

McMurry, P. H., M. Fink, H. Sakurai, M. R. Stolzenburg, R. L. Mauldin III, J. Smith, F. Eisele, et al. "A Criterion for New Particle Formation in the Sulfur-Rich Atlanta Atmosphere." *J. Geophys. Res.,* 110 (D22): D22S02/10. doi:10.1029/2005JD005901, 2005.

Nadykto, A. and F. Yu. "Amine's in the Earth's Atmosphere: A Density Functional Theory Study of the Thermochemistry of Pre-Nucleation Clusters," *Entropy* 13: 554-569, 2011.

Nel, A. "Air Pollution-Related Illness: Effects of Particles." *Science* 308 (5723): 804-806. doi:10.1126/science.1108752, 2005.

Ortega, I. K., O. Kupiainen, T. Kurten, T. Olenius, O. Wilkman, M. J. McGrath, V. Loukonen, and H. Vehkamaki. "From Quantum Chemical Formation Free Energies to Evaporation Rates." *Atmospheric Chemistry and Physics* 12 (1): 225-235. doi:10.5194/acp-12-225-2012, 2012.

Panta, B, W A Glasoe, J H Zollner, K K. Carlson, and D. R. Hanson "Computational Fluid Dynamics of a Cylindrical Nucleation Flow Reactor with Detailed Cluster Thermodynamics," *J. Phys. Chem. A* 116: 10122-10134. doi:10.1021/jp302444y, 2012.

Payne, W. A., L. J. Stief, and D. D. Davis. "A Kinetics Study of the Reaction of HO_2 with SO_2 and NO;" *J. Am. Chem. Soc.* 95: 7614-7619, 1973.

Sipilä, M.,

Berndt, T., Petaejae, **T.**, Brus, **D.**, Vanhanen, **J.** Stratmann, **F.**, Patokoski, **J.**, **Mauldin, L., Hyvärinen, A.-P., Lihavainen, H., and Kulmala, M.:** "The Role of Sulfuric Acid in Atmospheric Nucleation." *Science* 327: 1243-1246. doi:10.1126/science.1180315, 2010.

Sörgel, M., E. Regelin, H. Bozem, J. -M Diesch, F. Drewnick, H. Fischer, H. Harder, et al. "Quantification of the Unknown HONO Daytime Source and its Relation to NO_2." ***Atmos Chem Phys*** 11(20): 10433-10447. doi:10.5194/acp-11-10433-2011, 2011.

Viisanen, Y., M Kulmala, and A Laaksonen. "Experiments on Gas-Liquid Nucleation of Sulfuric Acid and Water." *Journal of Chemical Physics* 107 (3): 920-926. doi:10.1063/1.474445, 1997.

Verheggen, B. and M. Mozurkewich. "Determination of Nucleation and Growth Rates from Observation of a SO_2 Induced Atmospheric Nucleation Event." *J Geophys Res* 107, doi:10.1029/2001JD000683, 2002.

Formatted: Indent: Left: -0.1", Hanging: 0.2"

Deleted: lamora

Formatted: Subscript

Deleted: Lovejoy, E. R., Hanson, D. R.: Kinetics and Products of the Reaction SO3 + NH3 + M, J. Phys. Chem., 100, 4459, 1996.¶

Deleted: HO_2

Deleted: SO_2

Deleted: Winer, R Atkinson, and J Pitts Jr. "Rate Constants for the Reaction of HO_2 with HO_2, SO_2, CO, N_20, Trans-2-Butene, and 2,3-Dimethyl-2-Butene at 300 K."

Moved up [23]: *J. Phys. Chem.* 83, 1979.¶

Deleted: Graham, R.A., A

Deleted: Sipilae,

Moved up [20]: M.,

Deleted: T.

Deleted: .

Deleted: D.

Deleted: J.

Deleted: F.

Deleted: J.

Deleted: et al

Formatted: Font: Not Italic

Deleted:

Formatted: Subscript

Deleted: *Atmospheric Chemistry and Physics*

Deleted:

Formatted: Subscript

Wexler, A. S. and S. L. Clegg. "Atmospheric Aerosol Models for Systems Including the Ions H+, NH_4+, Na+, SO_4^{2-}, NO_3^-, Cl^-, Br^-, and H_2O." *J Geophys Res* 107 (D14): 4207. doi:10.1029/2001JD000451, 2002.

Wyslouzil, B. E., J. H. Seinfeld, R. C. Flagan, and K. Okuyama. "Binary Nucleation in Acid-Water Systems. II. Sulfuric Acid-Water and a Comparison with Methanesulfonic Acid-Water." *Journal of Chemical Physics* 94 (10): 6842-6850. doi:10.1063/1.460262, 1991.

Young, L. H., Benson, D. R., Kameel, F. R., Pierce, J. R., Junninen, H., Kulmala, M., and Lee, S.-H.: Laboratory studies of H_2SO_4/H_2O binary homogeneous nucleation from the SO_2+OH reaction: evaluation of the experimental setup and preliminary results, Atmos. Chem. Phys., 8, 4997–5016, doi:10.5194/acp-8-4997-2008, 2008.

Yu, H., L Dai, Y Zhao, V P. Kanawade, S N. Tripathi, X Ge, M Chen, and S.-Hu Lee. "Laboratory Observations of Temperature and Humidity Dependencies of Nucleation and Growth Rates of Sub-3 nm Particles." *J. Geophys. Res.: Atmospheres* 122 (3): 1919-1929. doi:10.1002/2016JD025619, 2017.

Yu, H, R McGraw, and S-H Lee. "Effects of Amines on Formation of Sub-3 Nm Particles and their Subsequent Growth." *Geophysical Research Letters* 39. doi:10.1029/2011GL050099, 2012.

Zollner, J. H., W. A. Glasoe, B. Panta, K. K. Carlson, P. H. McMurry, and D. R. Hanson. "Sulfuric Acid Nucleation: Power Dependencies, Variation with Relative Humidity, and Effect of Bases," *Atmospheric Chemistry and Physics* 12 (10): 4399-4411. doi:10.5194/acp-12-4399-2012, 2012.

Formatted: Subscript
Formatted: Subscript
Formatted: Superscript
Formatted: Subscript
Formatted: Superscript
Formatted: Superscript
Formatted: Superscript
Formatted: Subscript
Formatted: Indent: Left: -0.1", Hanging: 0.2"
Deleted: .
Formatted: Normal
Deleted: ¶

Figures and captions.

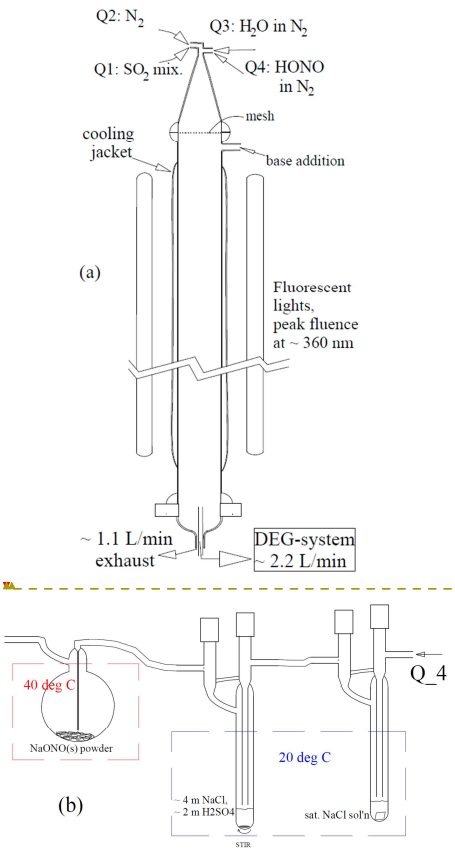

Fig. 1 (a) PhoFR schematic and (b) HONO source. The average flow velocity of 2.8 cm/s yields an average residence time in PhoFR of approximately 45 s. The concentrations listed in (b) are in molal (mole per kg H_2O).

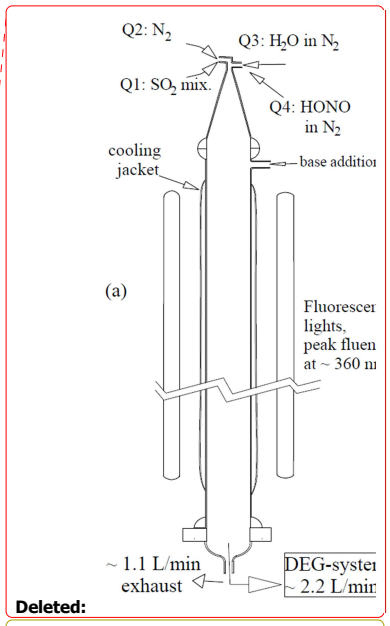

Deleted:

Formatted: Font: 10 pt, Not Bold

Formatted: Font: 10 pt, Not Bold

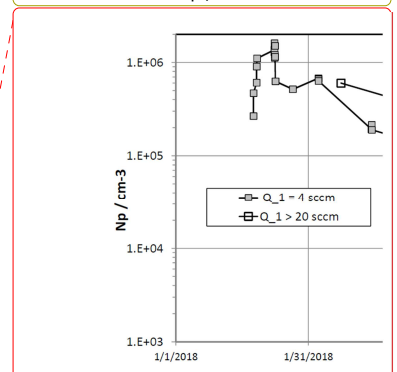

Deleted:

... [39]

Formatted: Font: 10 pt, Not Bold

Formatted: Font: 10 pt, Not Bold

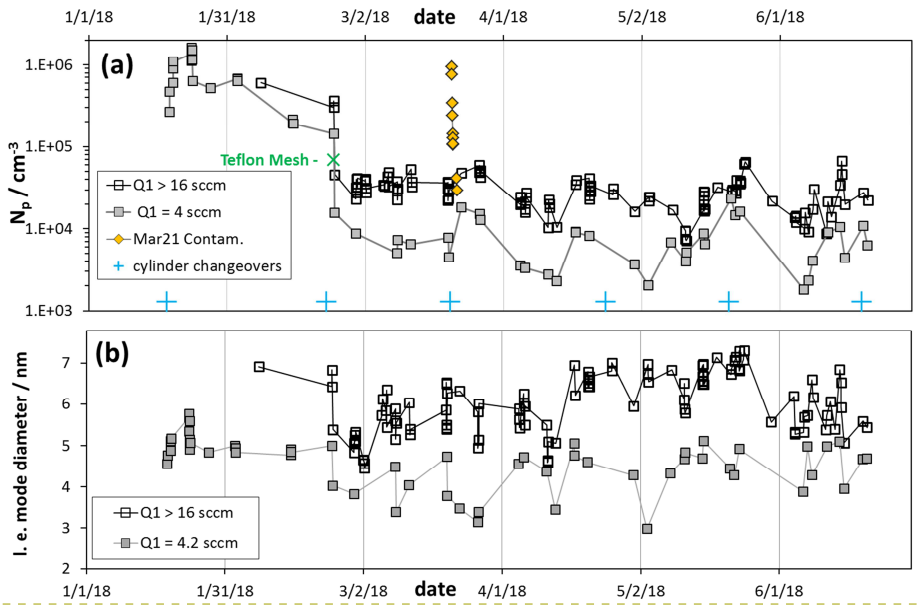

Fig. 2. (a) Number of large particles for baseline HONO (Q_4=4.2 sccm: [HONO] = 5x10^{11} cm^{-3}) plotted vs. time for two different SO_2 levels, equivalent to 2 and >8 ppmv. Data on 21 and 22 Mar are shown as the yellow diamonds and are for low SO_2 conditions: N_p is severely elevated due to a suspected dust contaminant. (b) Leading edge mode diameters plotted versus time also binned by SO_2 level.

Formatted: Font: 10 pt, Not Bold

Formatted: Right: 0.7"

Deleted: 10 ppmv. **(b) Measured size distributions for the high SO_2 conditions just after the mesh was installed, Feb. 23rd, and late in the time period depicted in (a).**

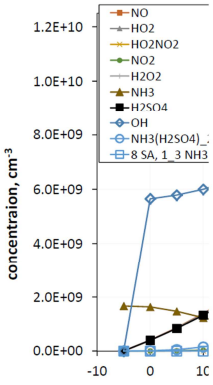

Deleted:

Formatted: Font: 10 pt, Not Bold

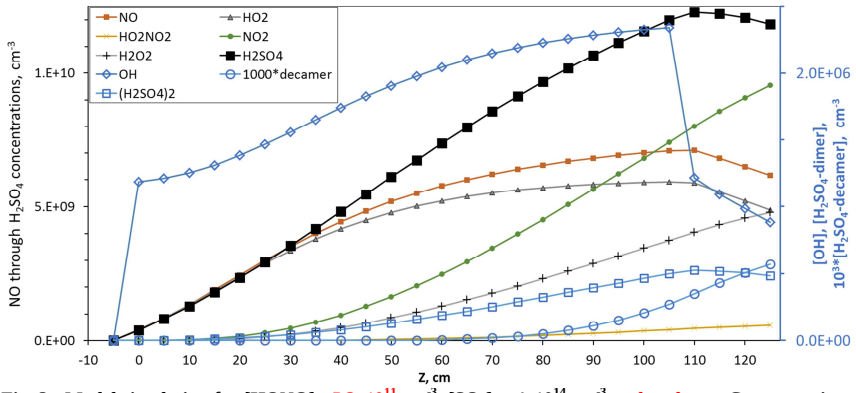

Fig. 3. Model simulation for [HONO]= 5.2x10^{11} cm^{-3}, [SO_2] = 4x10^{14} cm^{-3} and no base. Concentrations of NO through H_2SO_4 are plotted on the left axis; concentrations of OH and the $(H_2SO_4)_2$ and $(H_2SO_4)_{10}$ clusters on the right axis. These simulations are equivalent to experimental conditions of Q_4=4.2 sccm, Q_1= 32 sccm. The lighted section is from 0 to 110 cm. At 110 cm HONO photolysis ceases and [OH] (right axis) drops to a level supplied by HO_2 + NO.

Formatted: Right: 1"

Deleted: 5x10^{11}

Deleted: ,

Deleted: $_2NH_3$

Deleted: $_8(NH_3)_{1,2,3}$

Deleted: (the latter clusters were summed over NH_3 content and multiplied by 100).

Deleted: 0

Deleted: and added NH_3 at 70 pptv.

Deleted: <*object*>

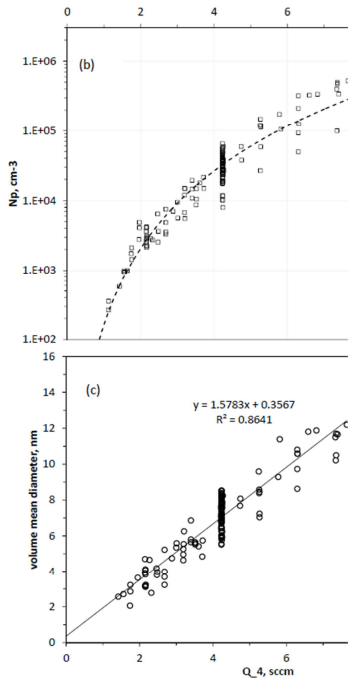

Fig. 4. (a) Measured size distributions as a function of Q_4, the flow rate through the HONO generator. Log-normal distributions manually fitted to the leading edge are shown as the dashed lines. Note that raw count rates at the smallest size for the three lowest Q_4 are roughly 0.1 s^{-1} and, statisticall ... [40]

Formatted: Font: 10 pt, Not Bold

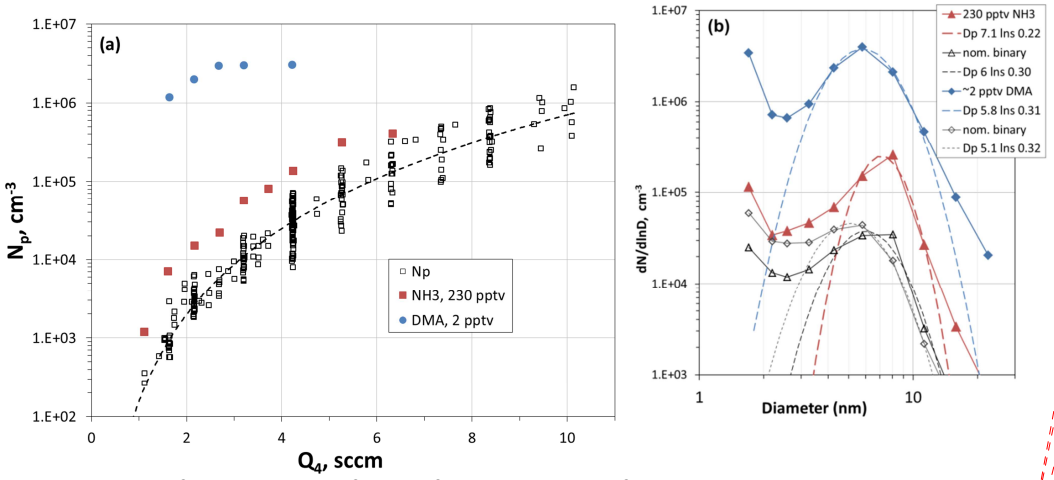

Fig. 4. (a) Number of large particles as a function of Q_4, the HONO-laden flow rate. RH was 52 %, T = 296 K, and $[SO_2] > 2.5x10^{14}$ cm^{-3}. For reference, Q_4 = 4.2 sccm results in a modeled value of ~ $4x10^9$ cm^{-3} for H_2SO_4 at Z = 35 cm and R = 0. Base-added experimental results are shown as the circles (dimethylamine) and red squares (ammonia). (b) Size distributions showing the effect of added NH_3 (red triangles) and added dimethylamine (blue diamonds). Nominal binary distributions for those runs are also shown. The log-normal distributions are also shown (dashed lines) and the legend indicates the mode diameter and lnσ in that order.

Formatted: Right: 0.4"

Deleted: (

Deleted: center of the reactor; see Fig. 3.) (c) Volume mean diameter of the particles in the leading edge of the particle

Deleted: , $D_{V,le} = D_{le}*\exp(1.5\ln\sigma^2)$. $D_{i,e}$ and lnσ from those

Deleted: had a local minimum between the smallest particles and the peak at large diameters and thus were able to be fit.

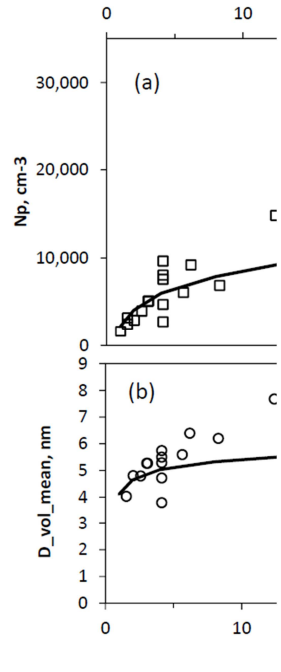

Deleted:

Formatted: Font: 10 pt

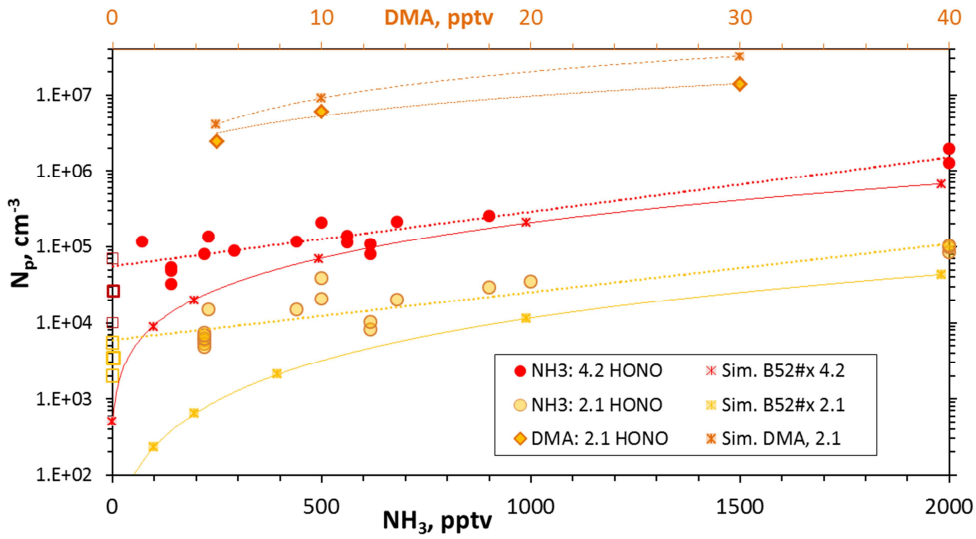

Fig. 5. Variation of measured N_p with added NH_3 for Q_4 of 4.2 sccm and 2.1 sccm and for added dimethylamine at Q_4 = 2.1 sccm (top axis for dimethylamine level). Simulated N_p are shown for NH3_52 (ammonia) and DMA_I (dimethylamine) thermodynamics. The average and the range of measured N_p without added base are shown as the squares for the two Q_4 levels.

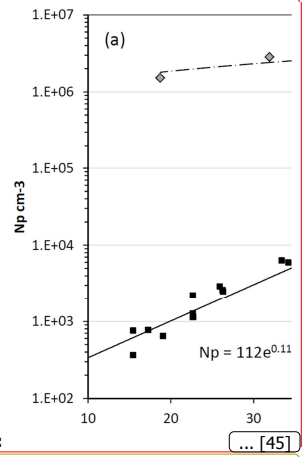

Formatted: Font: 10 pt, Not Bold

Deleted: Q_4, the HONO-source flow rate

Moved down [26]: Np vs.

Formatted: Right: 0.4"

Moved down [24]: flow rate of SO_2 mixture.

Moved down [25]: , was 4.2 sccm which results in roughly $5x10^{11}$ cm^{-3} [HONO] in PhoFR. ... [42]

Formatted: Font: 10 pt

Deleted: (a) Number of large particles and (b) volume mean ... [41]

Deleted: The orange lines are model values for N_p and size with ... [43]

Formatted: Not Superscript/ Subscript

Deleted: Q_4 (i.e., HONO) and (b) particle size distributions with NH_3 ... [44]

Formatted: Font: 10 pt

Deleted: N_p with

Deleted: NH_3

Deleted: Q_4 of (a) 4.3 sccm and (b) 2.2 sccm.

Formatted: Subscript

Deleted: in (a)

Deleted: and NH3_II

Deleted: ... [45]

Formatted: Font: 10 pt, Not Bold

Formatted: Font: 10 pt, Not Bold

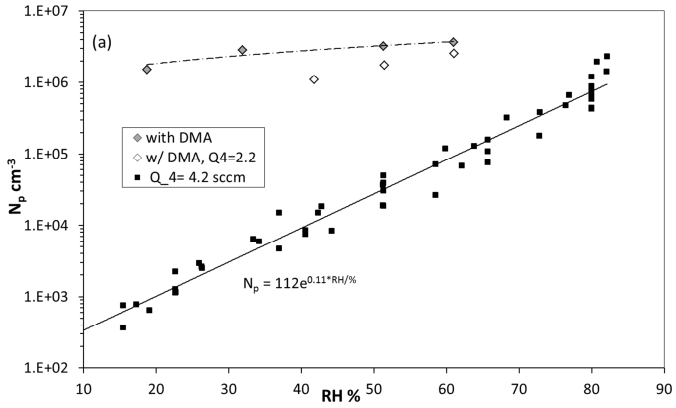

Fig. 6. Variation of N_p with RH in % (RH determined by the fraction of flow through the water saturator, Q_3) Q_4 was 4.2 sccm and Q_1 > 20 sccm. Also shown are data with dimethyl amine added: at 2 pptv (filled diamonds) and data at a lower Q_4 = 2.1 sccm and dimethyl amine at 5 pptv.

Deleted: 8.

Deleted: (a) N_p and (b) $D_{V,Ie}$ with

Deleted: Plot (a) also shows

Deleted: In (b) a linear fit is shown as the dashed line (phenomenological) while the solid line is the diameter increase based on water uptake using bulk values for the density and mass fraction of H_2SO_4 as a function of RH (Wexler and Clegg, 2002).

Formatted: Font: 10 pt, Not Bold

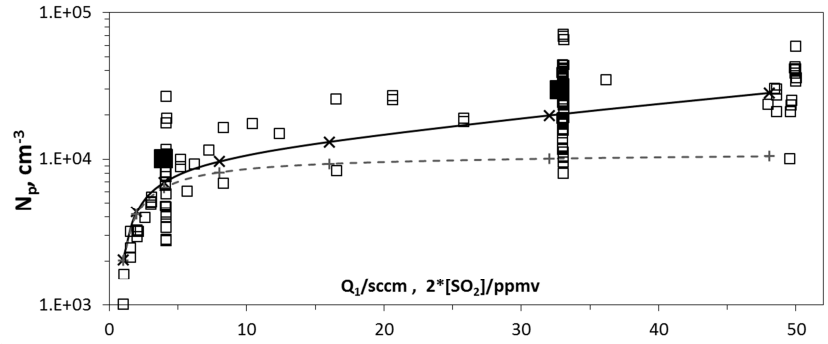

Fig. 7. Number of large particles vs. flow rate of SO_2 mixture. The HONO-source flow rate, Q_4, was 4.2 sccm which results in roughly 5x10^{11} cm^{-3} [HONO] in PhoFR. For reference, an SO_2 mixture flow rate of 32 sccm results in an [SO_2] of 4x10^{14} cm^{-3} in PhoFR (about 16 pptv). The solid and dashed lines are model values for N_p and size with 200 pptv NH_3 entering the flow reactor and a k3x5 (HO_2 + SO_2) rate coefficient of 3x10^{-17} cm^3/s (x's, solid lines) and in the absence of this reaction (+'s and dashed lines). The solid squares indicate the average at Q_1 = 4 and 32 sccm.

Moved (insertion) [24]

Moved (insertion) [25]

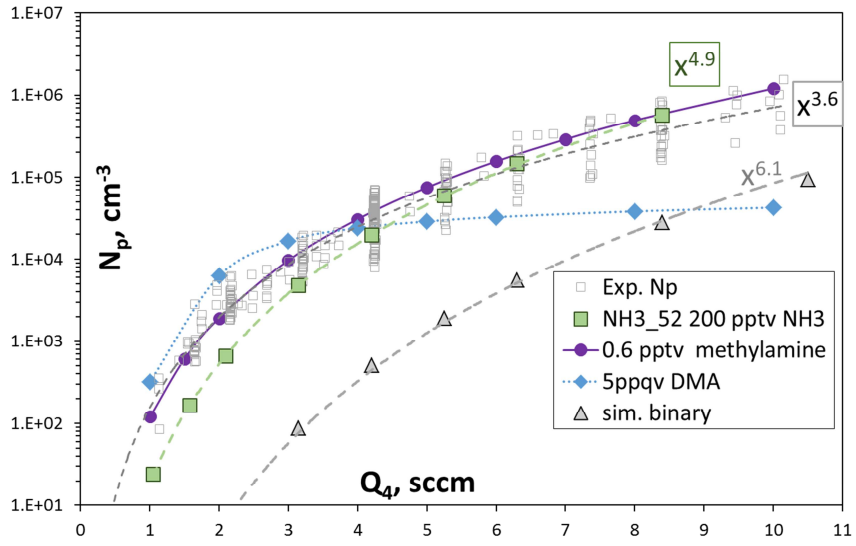

Figure 8. Np vs. Q_4, the HONO-containing flow. Experimental from Fig. 4(a), simulated is on-axis Np at axial position = 120 cm into PhoFR. Green symbols are ammonia at 200 pptv and the gray triangles are the binary, simulated with scheme NH3_52 thermodynamics; the blue diamonds are simulations with 0.005 pptv dimethylamine added using DMA_I thermodynamics. The purple circles are 0.6 pptv methylamine from Glasoe et al. (2015).

Moved (insertion) [26]

Formatted: Font: 10 pt, English (U.K.), Not Superscript/ Subscript

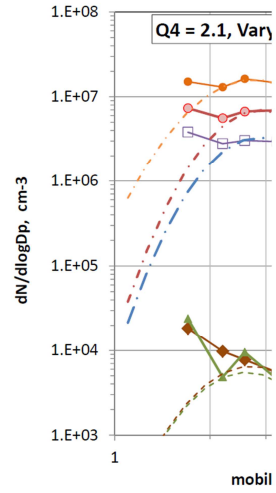

Deleted:

Fig. 9 Size distributions as a function of added dimethyl amine.

¶

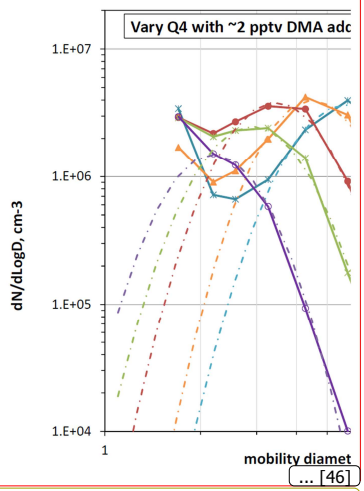

... [46]

Formatted: Font: 10 pt

Formatted: Font: 10 pt

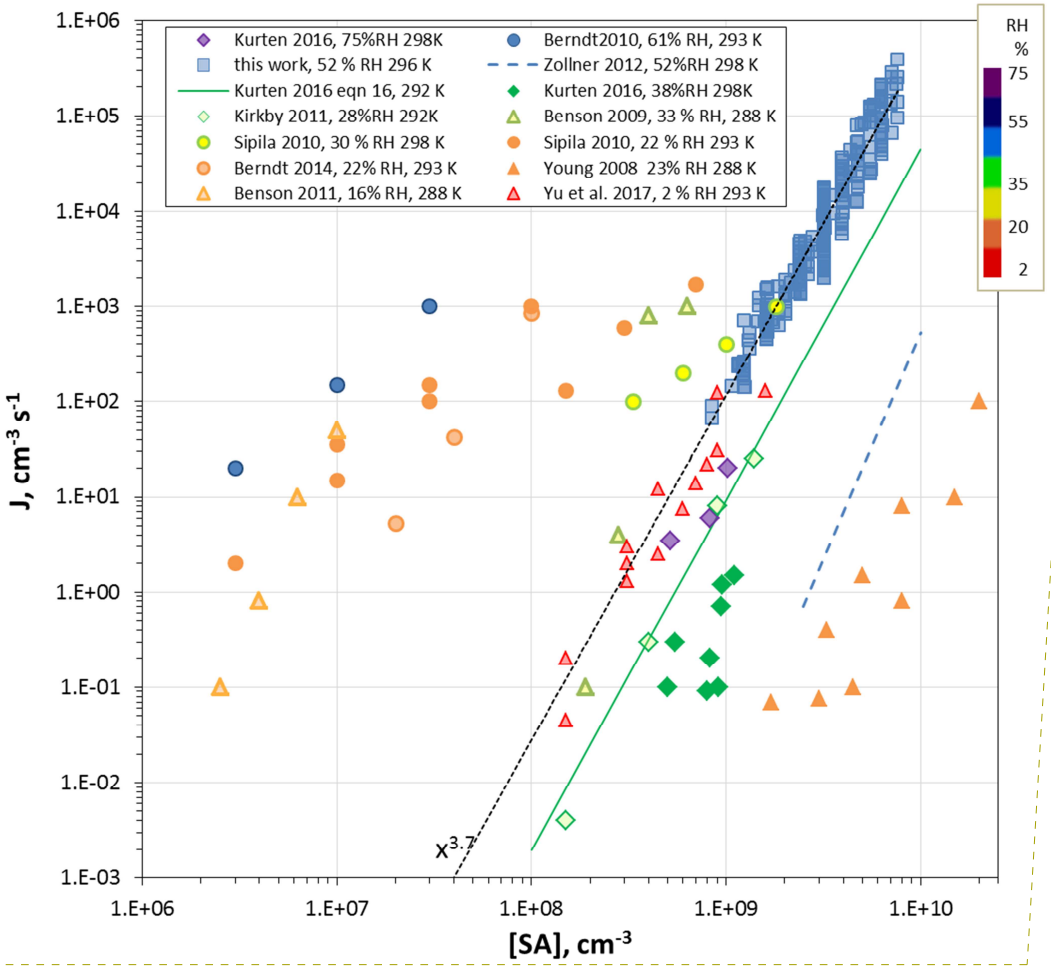

Fig. 9: Comparison of results from previous work (all photolytic H_2SO_4 production except Zollner et al., 2012) for nominally clean conditions. RH color-coding was applied to the points and temperatures are indicated in the legend.

Formatted: Font: 10 pt, Not Bold

Deleted: 11

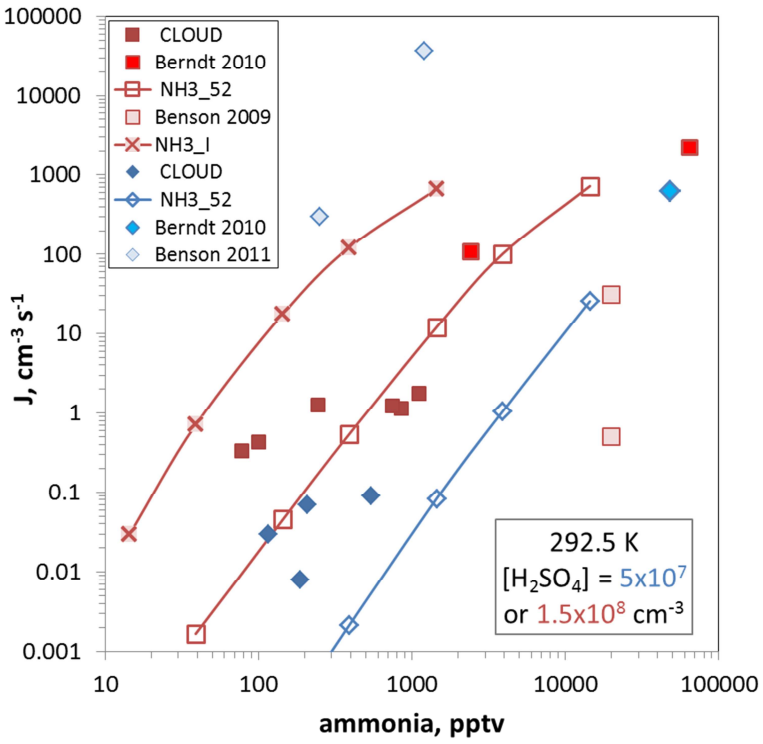

Fig. 10. Ammonia-sulfuric acid nucleation rate vs. ammonia abundance. Sulfuric acid level is $5x10^7$ cm^{-3} for the blue diamonds and $1.5x10^8$ cm^{-3} for the red squares. CLOUD data is from Dunne et al., 292.5 K, neutral conditions. Berndt et al. (2010), 293 K, has their squared dependence on $[H_2SO_4]$ applied which results in a division by ~30 to extrapolate to the $1.5x10^8$ cm^{-3} conditions; no corrections needed for the $5x10^7$ cm^{-3} data point. Benson et al. (2009) report a 4 power dependence on sulfuric acid and correction factors are 5 and divide by 16. Benson et al. (2011) requires multiplicative factors of ~40 to extrapolate to $5x10^7$ cm^{-3} $[H_2SO_4]$. Box model nucleation rates for the two different $[H_2SO_4]$ are shown for the NH3_52 thermodynamics and J for the $1.5x10^8$ cm^{-3} conditions was also predicted using NH3_I from Hanson et al. (2017).

Formatted: Font: 10 pt, Not Bold

Page 1: [1] Comment [R1] **Reviewer1** **6/11/2019 7:26:00 PM**

We agree with this point and believe this reviewer detailed this issue in their comment at the bottom of C4 regarding a more systematic presentation of the results. Indeed, we consolidated three size distributions into 1 figure (moving the majority of the data in these 3 distribution plots to the supplement) and we also consolidated two data sets into one figure where Np is plotted vs Q4.

Page 1: [2] Comment [R2] **Reviewer1** **6/11/2019 7:26:00 PM**

We have a new title (see next comment) and reworked the abstract to better summarize the added value of this work.

Page 1: [3] Comment [R3] **Reviewer1** **6/11/2019 7:26:00 PM**

New title: "H2SO4 and particle production in a Photolytic Flow Reactor. Chemical modeling, cluster thermodynamics and contamination issues "

Page 1: [4] Comment [R4] **Reviewer1** **6/11/2019 7:26:00 PM**

We added a paragraph on uncertainties in Supplement S4. The bottom line is that random uncertainties are small and scatter is likely due to (small ?) temperature fluctuations. This comment also prompted us to add a section (S1.0) to the Supplement showing raw data from a typical run and a table that shows the correction factors.

Page 15: [5] Deleted **Reviewer1** **6/11/2019 4:19:00 PM**

NH_3 was introduced at the inlet at a level of 70 pptv which drops with axial distance due to wall loss: its concentration drops to ~20 % of the inlet value by 40 cm.

Page 15: [6] Deleted **Reviewer1** **6/11/2019 4:19:00 PM**

effect of added base on particle formation is primarily at the top

Page 15: [7] Deleted **Reviewer1** **6/11/2019 4:19:00 PM**

despite the lowest sulfuric acid abundances there. The remaining 2/3 of the reactor has

Page 15: [8] Deleted **Reviewer1** **6/11/2019 4:19:00 PM**

This crude partitioning of

Page 15: [9] Deleted **Reviewer1** **6/11/2019 4:19:00 PM**

Modeled particles that contain up to 250 H_2SO_4 molecules yield particle size distributions in agreement with this estimate from bulk properties (see the Supplement).

Page 15: [10] Deleted **Reviewer1** **6/11/2019 4:19:00 PM**

shown in Fig. 3 provides some justification

Page 15: [11] Deleted **Reviewer1** **6/11/2019 4:19:00 PM**

/3. The abundance of $(H_2SO_4)_2NH_3$ peaks at about 50 cm indicating that

Page 15: [12] Deleted **Reviewer1** **6/11/2019 4:19:00 PM**

involving base has reached its peak. The accumulation cluster (that was allowed to build up at 8 SA molecules but no further and with no SA evaporation) tells a similar story regarding this partitioning where its abundance levels off in the lower section

Page 16: [13] Deleted **Reviewer1** **6/11/2019 4:19:00 PM**

4c and is probably affected by the inability of the fitting process (see Supplement) to yield leading edge log-normal distributions at low values of Q_4 (indeed about half failed for $Q_4 \leq 2.2$ sccm) and scavenging of H_2SO_4 by particle surface area at the large N_p that develops at high number densities and large sizes when Q_4 is 8 to 10 sccm.

Page 17: [14] Deleted **Reviewer1** **6/11/2019 4:19:00 PM**

2013) show that power dependencies on H_2SO_4 are affected when a base is present. The presence of an impurity base compound probably affected our experimental results. It may be due to two sources: (i) contaminant entering with the flows and (ii) contaminant emanating from internal surfaces. The added base experiments have more discussion on this topic but we note here that our system is slowly cleaning up over time.

Particles grow due to uptake of H_2SO_4 and H_2O: the estimate from the H_2SO_4 profile from the model simulation discussed above suggests an increase in diameter of about 4.8 nm for a Q_4 of 4.0 sccm. The data in Fig. 4c show that the volume mean diameter is about 6 nm at this HONO level, which is consistent with that estimate. The agreement improves considering that nascent particles must attain a certain size to become stable, roughly 1.3 nm diameter or larger (large enough such that evaporation becomes negligible). There is also a 0.3 nm difference between mobility and volume/mass diameters. Presented in the Supplement are simulated particle size distributions for Q_4= 2 sccm that peak at 3.7 nm in good agreement with measurements.

3.2.2

Page 17: [15] Deleted **Reviewer1** **6/11/2019 4:19:00 PM**

Figs. 5 (a) and (b) are plots of N_p and $D_{V,le}$ (volume mean diameter of the leading-edge mode) vs.

Page 17: [16] Moved to page 20 (Move #8) **Reviewer1** **6/11/2019 4:19:00 PM**

the flow rate of the SO_2 mixture, Q_1. HONO source flow rate Q_4 was 4.2 sccm for this data. Despite its scatter, the data show the SO_2 level affects both the number of large particles and their size, $D_{V,le}$

Page 17: [17] Deleted **Reviewer1** **6/11/2019 4:19:00 PM**

: both increase with [SO_2] and begin to level-off at high [SO_2]. This behavior is expected as the SO_2 abundance must be high enough to ensure it scavenges all of the OH and beyond that there should not be much effect.

However, a set of simulations that includes a reaction between HO_2 and SO_2 are shown as the lines in Figs. 5. Note that a level of 70 pptv of NH_3 entering the flow reactor was included. The simulated size is given by the growth estimate from the simulated H_2SO_4 profile plus an initial size of 1 nm and the mobility-diameter to mass-diameter offset of 0.3 nm (de La Mora et al.)

Page 17: [18] Moved to page 20 (Move #9) **Reviewer1** **6/11/2019 4:19:00 PM**

The experimental results show increases with SO_2 that are roughly in line with the model simulations.

Page 17: [19] Deleted **Reviewer1** **6/11/2019 4:19:00 PM**

Without a reaction between HO_2 and SO_2, the model shows small increases in N_p (40 % vs. 250 % with the reaction) and size (10% vs. 20 % with the reaction) as SO_2 was increased from 2 to 16 pptv.

Page 17: [20] Moved to page 20 (Move #10) **Reviewer1** **6/11/2019 4:19:00 PM**

The simulation assumed a value of $3x10^{-17}$ cm^3/s for $k_{HO2+SO2}$.

Page 17: [21] Moved to page 21 (Move #11) Reviewer1 6/11/2019 4:19:00 PM

whether HO_2 reacts with SO_2 as well as potential end products (Chen et al. 2014; Kurten et al. 2011); we assumed H_2SO_4 and OH.

Page 17: [22] Moved to page 21 (Move #12) Reviewer1 6/11/2019 4:19:00 PM

values for this rate coefficient range from upper limits of $1x10^{-18}$ cm^3/s (Graham et al. 1979) and $2x10^{-17}$ cm^3/s (Burrows et al. 1979), to a value of $8x10^{-16}$ cm^3/s (Payne et al. 1973). A heterogeneous reaction occurring in the particles involving SO_2 would help explain the dependence of $D_{V,le}$ on SO_2 abundance

Page 17: [23] Deleted Reviewer1 6/11/2019 4:19:00 PM

while leaving N_p undisturbed.

The dependencies upon SO_2 were much smaller when minute amounts of dimethylamine were included in the model. Low levels of (0.003 pptv) dimethylamine gave simulated N_p in the 10^4 cm^{-3} range but at this level its ability to influence the change in N_p with H_2SO_4 was limited due to being scavenged by clusters. This was also observed in simulations where HONO was varied in the presence of 0.005 pptv dimethylamine (see the Supplement). This suggests that a potential contaminant in our system is not a strong nucleator like dimethylamine.

3.2.3 Added ammonia.

Page 17: [24] Deleted Reviewer1 6/11/2019 4:19:00 PM

6 is the number of large particles vs. HONO flow rate taken with and without NH_3 addition. The level of

Page 17: [24] Deleted Reviewer1 6/11/2019 4:19:00 PM

6 is the number of large particles vs. HONO flow rate taken with and without NH_3 addition. The level of

Page 17: [24] Deleted Reviewer1 6/11/2019 4:19:00 PM

6 is the number of large particles vs. HONO flow rate taken with and without NH_3 addition. The level of

Page 17: [24] Deleted Reviewer1 6/11/2019 4:19:00 PM

6 is the number of large particles vs. HONO flow rate taken with and without NH_3 addition. The level of

Page 17: [25] Deleted Reviewer1 6/11/2019 4:19:00 PM

nominal

Page 17: [25] Deleted Reviewer1 6/11/2019 4:19:00 PM

nominal

Page 17: [25] Deleted Reviewer1 6/11/2019 4:19:00 PM

nominal

Page 17: [25] Deleted Reviewer1 6/11/2019 4:19:00 PM

nominal

Page 17: [25] Deleted **Reviewer1** **6/11/2019 4:19:00 PM**

nominal

Page 17: [25] Deleted **Reviewer1** **6/11/2019 4:19:00 PM**

nominal

Page 17: [25] Deleted **Reviewer1** **6/11/2019 4:19:00 PM**

nominal

Page 17: [25] Deleted **Reviewer1** **6/11/2019 4:19:00 PM**

nominal

Page 17: [25] Deleted **Reviewer1** **6/11/2019 4:19:00 PM**

nominal

Page 17: [25] Deleted **Reviewer1** **6/11/2019 4:19:00 PM**

nominal

Page 17: [25] Deleted **Reviewer1** **6/11/2019 4:19:00 PM**

nominal

Page 17: [25] Deleted **Reviewer1** **6/11/2019 4:19:00 PM**

nominal

Page 17: [25] Deleted **Reviewer1** **6/11/2019 4:19:00 PM**

nominal

Page 17: [26] Deleted **Reviewer1** **6/11/2019 4:19:00 PM**

For example

Page 17: [26] Deleted **Reviewer1** **6/11/2019 4:19:00 PM**

For example

Page 17: [26] Deleted **Reviewer1** **6/11/2019 4:19:00 PM**

For example

Page 17: [26] Deleted **Reviewer1** **6/11/2019 4:19:00 PM**

For example

Page 17: [26] Deleted **Reviewer1** **6/11/2019 4:19:00 PM**

For example

Page 17: [26] Deleted **Reviewer1** **6/11/2019 4:19:00 PM**

For example

Page 17: [26] Deleted **Reviewer1** **6/11/2019 4:19:00 PM**

For example

Page 17: [26] Deleted **Reviewer1** **6/11/2019 4:19:00 PM**

For example

Page 17: [26] Deleted	Reviewer1	6/11/2019 4:19:00 PM

For example

Page 20: [27] Deleted	Reviewer1	6/11/2019 4:19:00 PM

3.2.6 Variations of dimethylamine and HONO.

Shown in Fig. 9 are measured size distributions with varying levels of added dimethylamine. The effect on the number of particles is large and even the smallest particles (mobility diameter of 1.7 nm) increased by about 3 orders of magnitude. The zero-added base data between these runs might be affected by dimethylamine holdover but this appears to be small: the N_p are within a factor of two of the Q_4=2.2 sccm data in Fig. 4a. It is clear that more dimethylamine leads to more particles, with N_p increasing approximately linearly with dimethylamine abundance. Note that the leading edge of the distributions is clearly the dominant mode for these conditions. The D_{le} does not change significantly with the amount of added dimethyl amine (see the legend for values of D_{le} and $\ln\sigma_{le}$).

Depicted in Fig. 10 are results from an experiment where HONO, Q_4, was varied (and thus H_2SO_4) in the presence of 2 pptv (+100/-50%) dimethylamine. Interestingly, the number of particles is not particularly sensitive to H_2SO_4 above Q_4 = 2.7 sccm while their size is linearly dependent on Q_4. The model indicates a leveling off in the calculated N_p as Q_4 increases (see the Supplement) which appears to be due to scavenging of the amine by particles. Another contributing factor to an insensitivity of particle number concentrations to H_2SO_4 is particle-particle collisions. A rough estimate of these effects, assuming a coagulation rate coefficient of $2x10^{-9}$ cm^3/s, for an N_p of $4x10^6$ cm^{-3} is $2x10^{-9}*(4x10^6)^2 = 3x10^4$ cm^{-3} s^{-1} ; multiplying by a 30 s residence time and roughly $1x10^6$ cm^{-3} would coagulate. This rough estimate suggests the effect should be properly evaluated, particularly for the data presented in Fig. 9. Note also that these are small sets of data and for Fig. 10 base was added at a level that challenges the lower range of the dynamic dilution system.

Model

Page 24: [28] Deleted	Reviewer1	6/11/2019 4:19:00 PM

3 (Kurten et al., 2017), albeit at lower H_2SO_4. At constant NH_3, we found power dependencies on H_2SO_4 for N_p of about 3.5 which is close to

Page 24: [29] Deleted	Reviewer1	6/11/2019 4:19:00 PM

found by Glasoe et al. (2015) and somewhat larger than the CLOUD data (H_2SO_4-power dependency of 2.6.) A linear dependence on

Page 24: [30] Deleted	Reviewer1	6/11/2019 4:19:00 PM

nucleation initiated by sulfamic acid, as outlined by Lovejoy and Hanson (1996).

Page 24: [31] Deleted	Reviewer1	6/11/2019 4:19:00 PM

exceeded experiment for a large set of conditions.

Page 24: [32] Deleted **Reviewer1** **6/11/2019 4:19:00 PM**

., but now, since the Glasoe et al. data are higher than the latter two as well as for much of

Page 24: [33] Deleted **Reviewer1** **6/11/2019 4:19:00 PM**

, we conclude that the Glasoe et al. NH_3 results are biased high. Finally, the putative agreement between Glasoe et al. and the 292 K 4 pptv NH_3 data from CLOUD (demonstrated in Fig. 4 of Kurten et al. 2016) should not be a validation of these two sets of NH_3-H_2SO_4 nucleation rates.

Page 24: [34] Deleted **Reviewer1** **6/11/2019 4:19:00 PM**

would be most vulnerable to the presence of small amounts of holdover amines.

Page 24: [35] Deleted **Reviewer1** **6/11/2019 4:19:00 PM**

investigated with a proper coagulation simulation

Page 24: [36] Deleted **Reviewer1** **6/11/2019 4:19:00 PM**

investigation. Furthermore, we conclude that the

Page 24: [37] Deleted **Reviewer1** **6/11/2019 4:19:00 PM**

likely overestimates nucleation in the ammonia-sulfuric acid system.

Page 24: [38] Deleted **Reviewer1** **6/11/2019 4:19:00 PM**

to better determine H_2SO_4 and amine dependencies.

Page 31: [39] Deleted **Reviewer1** **6/11/2019 4:19:00 PM**

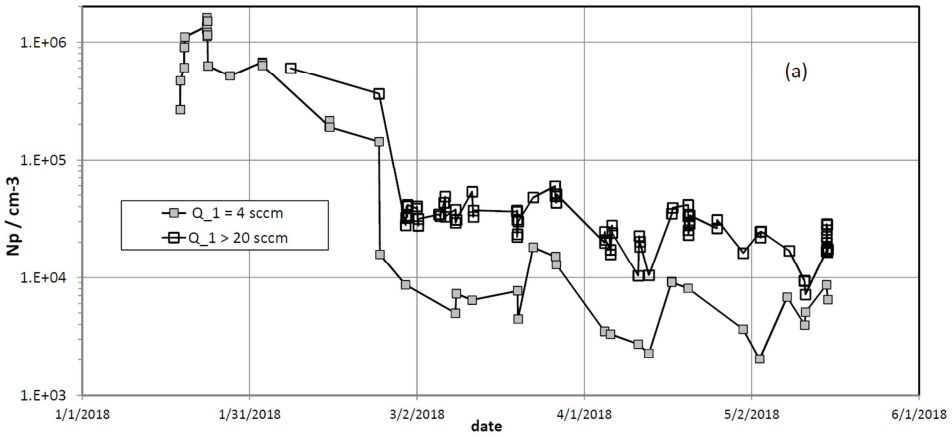

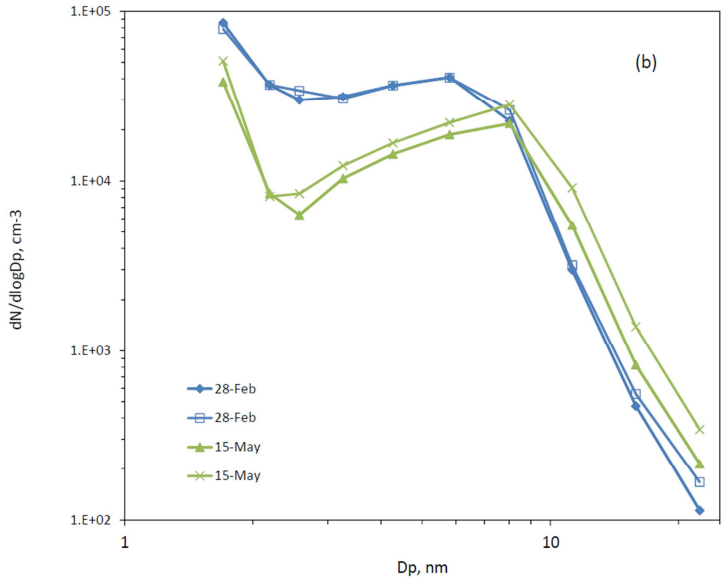

Page 33: [40] Deleted **Reviewer1** **6/11/2019 4:19:00 PM**

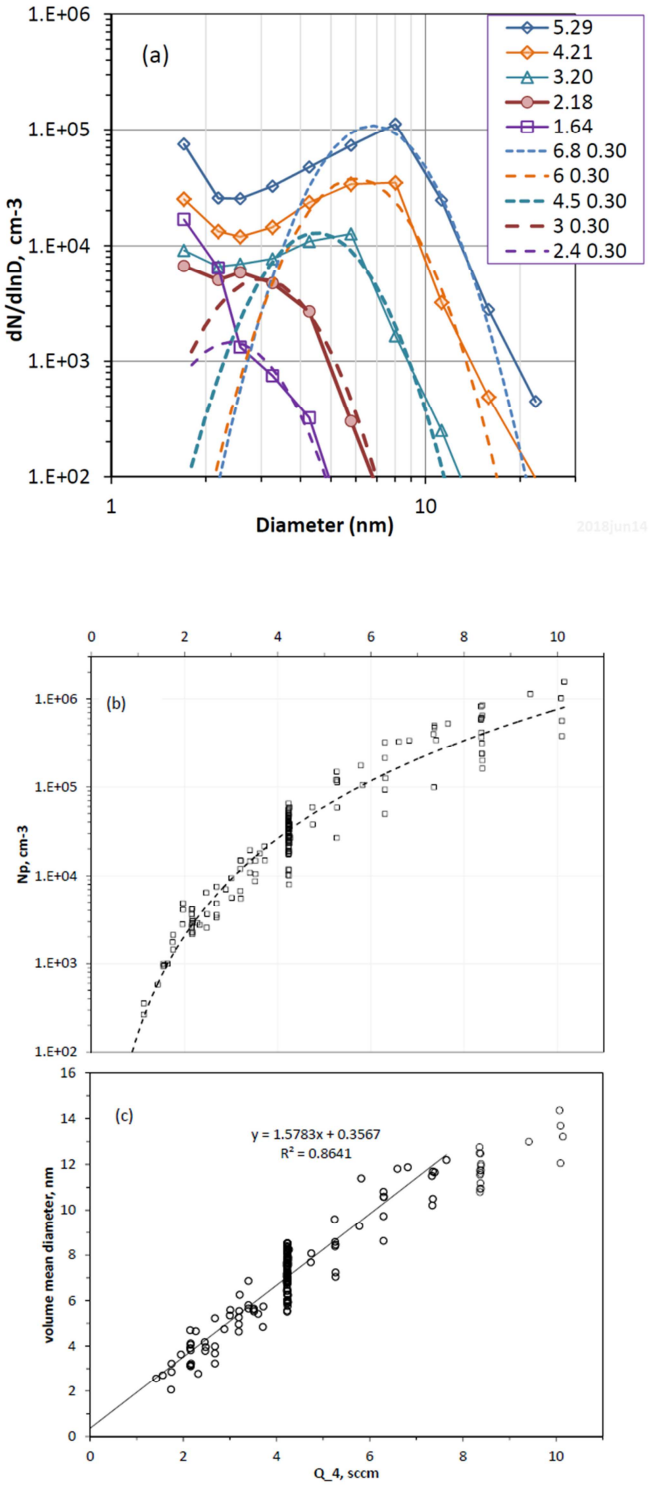

Fig. 4. (a) Measured size distributions as a function of Q_4, the flow rate through the HONO generator. Log-normal distributions manually fitted to the leading edge are shown as the dashed lines. Note that raw count rates at the smallest size for the three lowest Q_4 are roughly 0.1 s^{-1} and, statistically, they are not significantly different. This is slightly above the background count rate of ~0.05 s^{-1}. (b

Page 35: [41] Deleted **Reviewer1** **6/11/2019 4:19:00 PM**

(a) Number of large particles and (b) volume mean diameter of the leading edge mode plotted vs.

Page 35: [42] Moved to page 36 (Move #25) **Reviewer1** **6/11/2019 4:19:00 PM**

, was 4.2 sccm which results in roughly 5x10^{11} cm^{-3} [HONO] in PhoFR. For reference, an SO_2 mixture flow rate of 32 sccm results in an [SO_2] of 4x10^{14} cm^{-3} in PhoFR (about 16 pptv).

Page 35: [43] Deleted **Reviewer1** **6/11/2019 4:19:00 PM**

The orange lines are model values for N_p and size with 70 pptv NH_3 entering the flow reactor and a k3x5 (HO_2 + SO_2) rate coefficient of 3x10^{-17} cm^3/s. The simulated size has 1.3 nm (to take into account initial cluster size of ~ 1 nm and the mobility to mass size difference of 0.3 nm. de La Mora et al.) added to the growth due to H_2SO_4 exposure as discussed above.

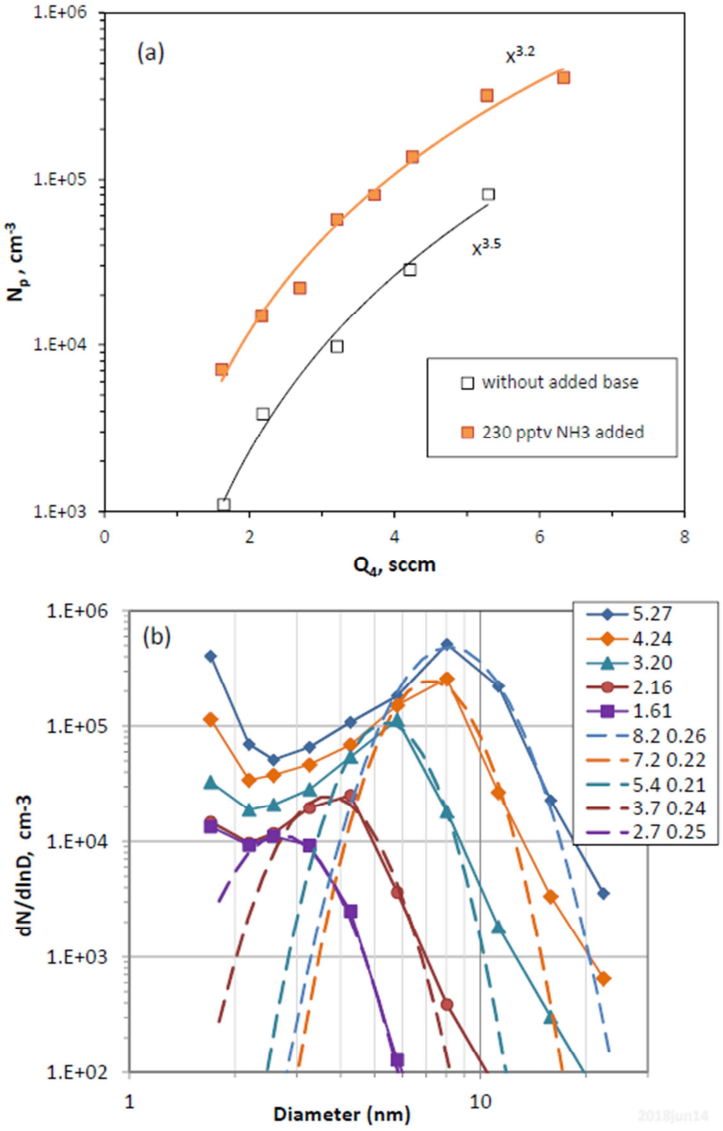

Fig. 6 (a)

Page 35: [44] Deleted	Reviewer1	6/11/2019 4:19:00 PM

Q_4 (i.e., HONO) and (b) particle size distributions with NH_3 present. In (b), the log-normal parameters are listed in the legend and were obtained from a fitting procedure except for the Q_4 = 1.61 sccm data.

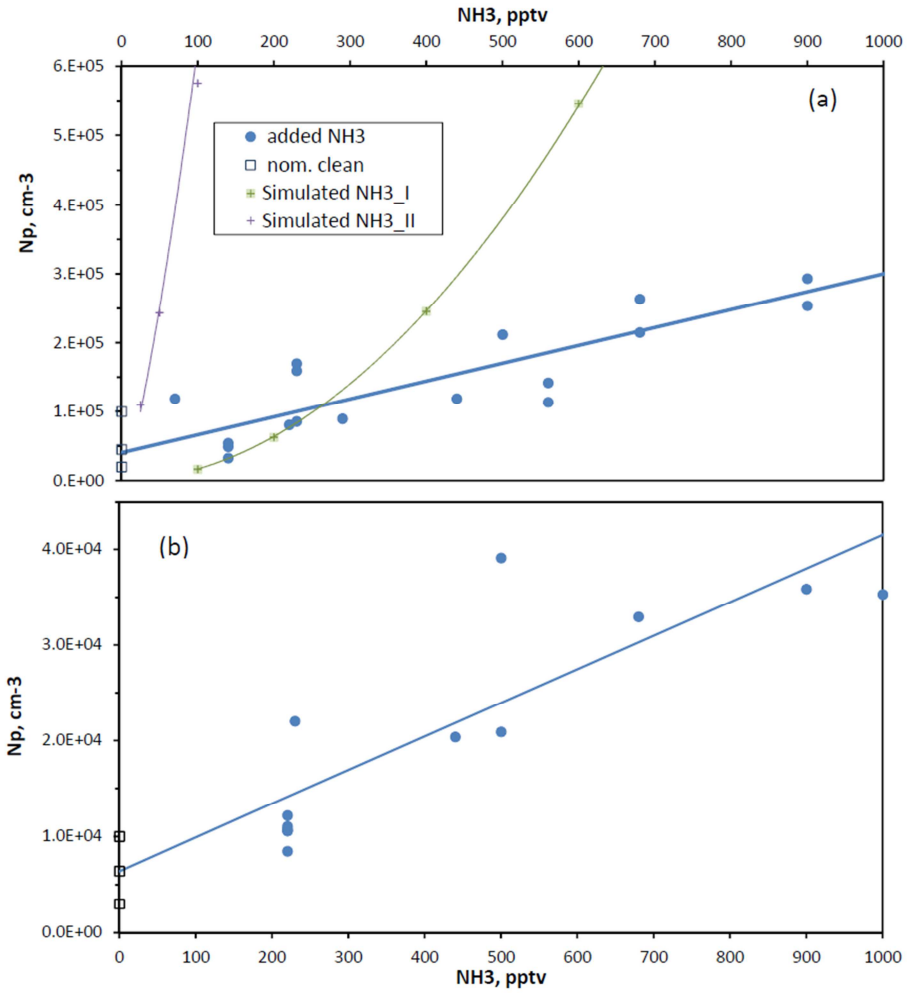

Fig. 7

Page 35: [45] Deleted	Reviewer1	6/11/2019 4:19:00 PM

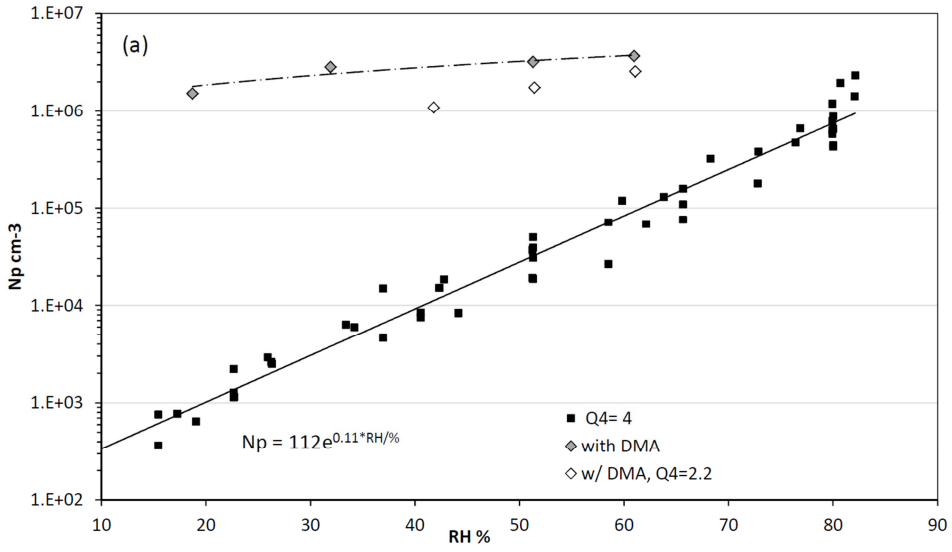

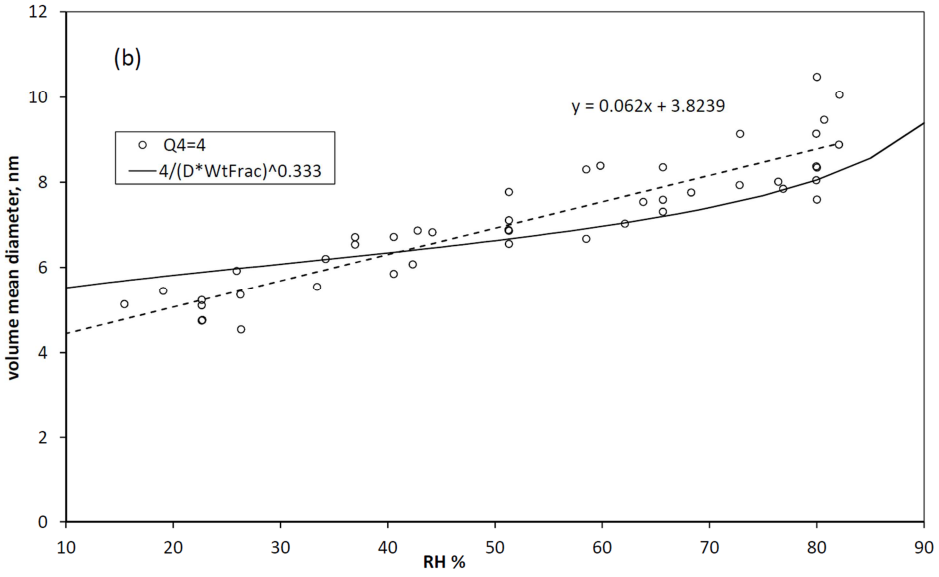

Page 37: [46] Deleted **Reviewer1** **6/11/2019 4:19:00 PM**

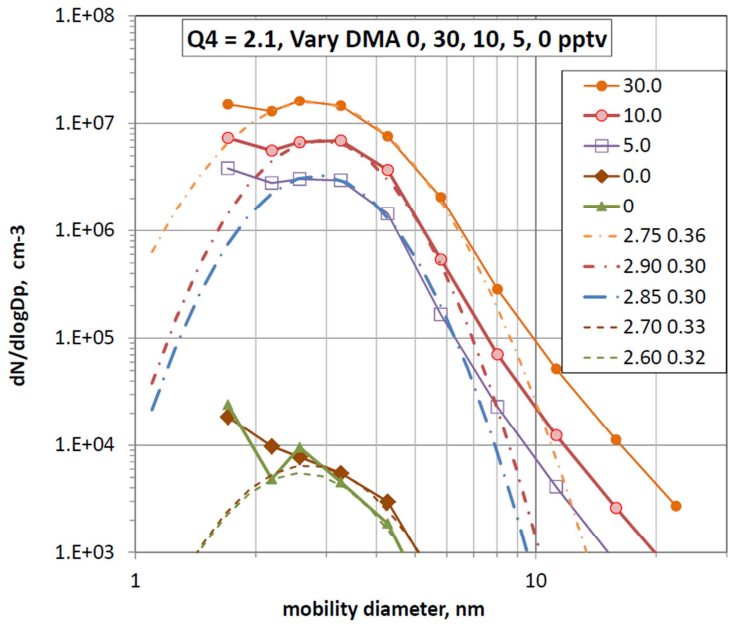

Fig. 9 Size distributions as a function of added dimethyl amine.

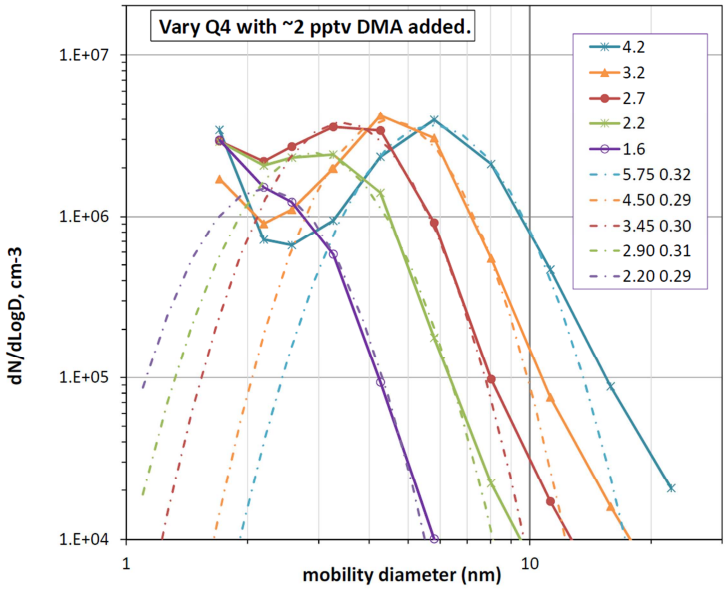

Fig. 10. Size distributions as a function of HONO level.

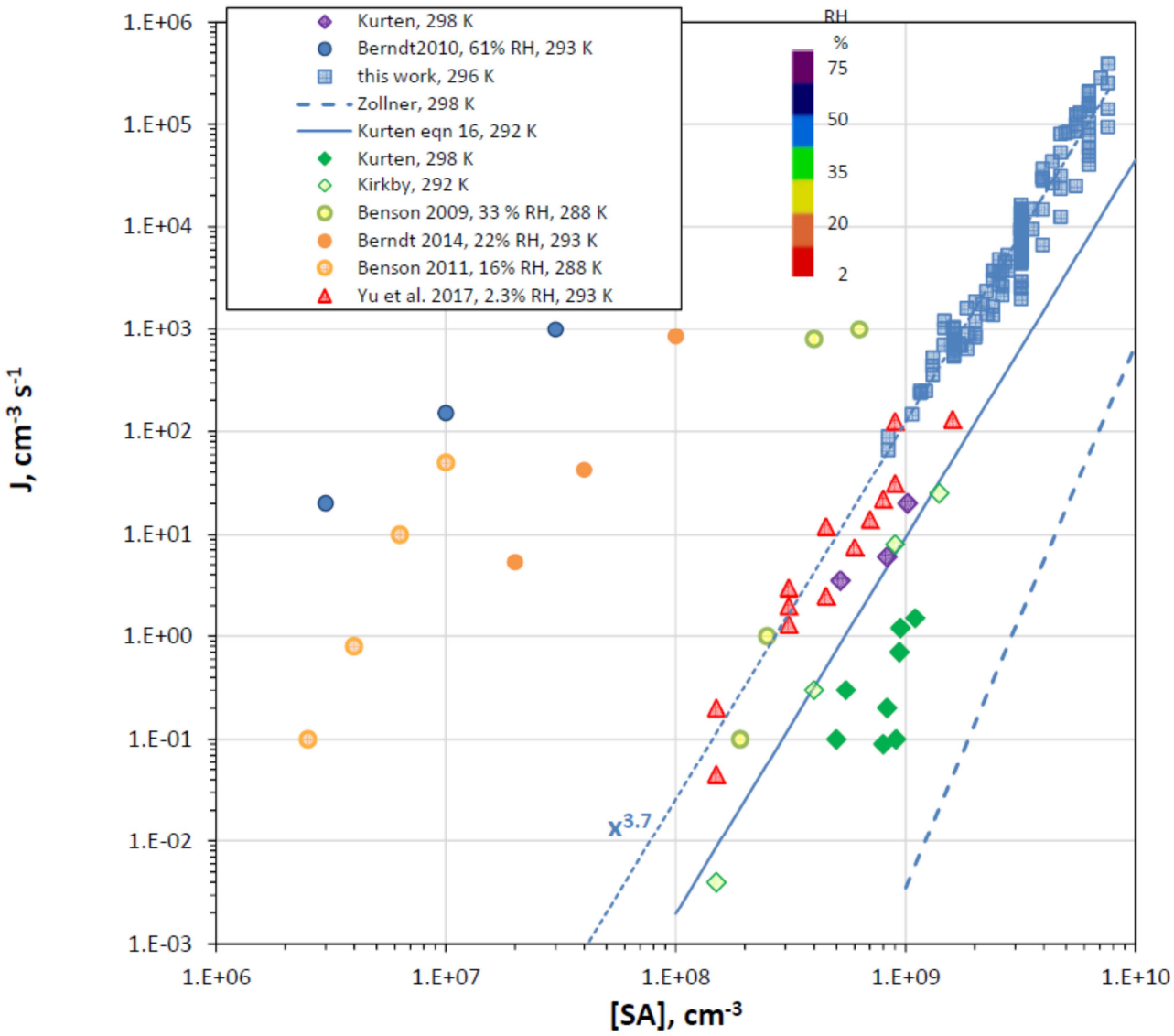
Kurten, 298 K
Berndt2010, 61% RH, 293 K
this work, 296 K
Zollner, 298 K
Kurten eqn 16, 292 K
Kurten, 298 K
Kirkby, 292 K
Benson 2009, 33 % RH, 288 K
Berndt 2014, 22% RH, 293 K
Benson 2011, 16% RH, 288 K
Yu et al. 2017, 2.3% RH, 293 K
RH
%
75
50
35
20
2
x3.7
J, cm-3 s-1
[SA], cm-3
1.E+06
1.E+05
1.E+04
1.E+03
1.E+02
1.E+01
1.E+00
1.E-01
1.E-02
1.E-03
1.E+06
1.E+07
1.E+08
1.E+09
1.E+10